PHOTOGRAPH THIS SHEET

AD-A198 639

DTIC ACCESSION NUMBER

LEVEL

1

INVENTORY

ESL 784460-8

DOCUMENT IDENTIFICATION

JAN 1979

This document has been approved for public release and sale; its distribution is unlimited.

DISTRIBUTION STATEMENT

ACCESSION FOR	
NTIS	GRA&I ☒
DTIC	TAB ☐
UNANNOUNCED	☐
JUSTIFICATION	per form 50
BY	
DISTRIBUTION /	
AVAILABILITY CODES	
DIST	AVAIL AND/OR SPECIAL
A-1	

DISTRIBUTION STAMP

DTIC
ELECTE
SEP 19 1988
S D
E

DATE ACCESSIONED

DATE RETURNED

88 9 16 239

DATE RECEIVED IN DTIC

REGISTERED OR CERTIFIED NO.

PHOTOGRAPH THIS SHEET AND RETURN TO DTIC-FDAC

DTIC FORM 70A
MAR 86

DOCUMENT PROCESSING SHEET

PREVIOUS EDITION MAY BE USED UNTIL STOCK IS EXHAUSTED.

CHARACTERISTICS OF A VIDEO PULSE RADAR SYSTEM OPERATING IN THE HIGH FREQUENCY WINDOW AT THE HAZEL A MINE NEAR GOLD HILL, COLORADO

C. W. Davis, III and L. Peters, Jr.

The Ohio State University

ElectroScience Laboratory

Department of Electrical Engineering
Columbus, Ohio 43212

Technical Report 784460-8

January 1979

Contract DAAG53-76-C-0179

Department of the Army
US Army Mobility Equipment Research and Development Command
Ft. Belvoir, Virginia 22060

UNCLASSIFIED

SECURITY CLASSIFICATION OF THIS PAGE *(When Data Entered)*

REPORT DOCUMENTATION PAGE		READ INSTRUCTIONS BEFORE COMPLETING FORM
1. REPORT NUMBER	2. GOVT ACCESSION NO.	3. RECIPIENT'S CATALOG NUMBER
4. TITLE *(and Subtitle)* CHARACTERISTICS OF A VIDEO PULSE RADAR SYSTEM OPERATING IN THE HIGH FREQUENCY WINDOW AT THE HAZEL A MINE NEAR GOLD HILL, COLORADO		5. TYPE OF REPORT & PERIOD COVERED Technical Report 6. PERFORMING ORG. REPORT NUMBER ESL 784460-8
7. AUTHOR(s) C. W. Davis, III and L. Peters, Jr.		8. CONTRACT OR GRANT NUMBER(s) DAAG53-76-C-0179
9. PERFORMING ORGANIZATION NAME AND ADDRESS The Ohio State University ElectroScience Laboratory, Department of Electrical Engineering, Columbus, Ohio 43212		10. PROGRAM ELEMENT, PROJECT, TASK AREA & WORK UNIT NUMBERS
11. CONTROLLING OFFICE NAME AND ADDRESS Dept. of the Army, US Army Mobility Equipment Research and Development Command Ft. Belvoir, Virginia 22060		12. REPORT DATE January 1979 13. NUMBER OF PAGES 47
14. MONITORING AGENCY NAME & ADDRESS*(if different from Controlling Office)*		15. SECURITY CLASS. *(of this report)* Unclassified 15a. DECLASSIFICATION/DOWNGRADING SCHEDULE

16. DISTRIBUTION STATEMENT *(of this Report)*

17. DISTRIBUTION STATEMENT *(of the abstract entered in Block 20, if different from Report)*

18. SUPPLEMENTARY NOTES

19. KEY WORDS *(Continue on reverse side if necessary and identify by block number)*

Video pulse radar
Tunnel scattering
Radar measurements
Grey level plots
Underground void

20. ABSTRACT *(Continue on reverse side if necessary and identify by block number)*

This report describes the results obtained using a Video Pulse Radar System operating in the High Frequency Window to detect a tunnel in a granite medium to depths of 20 feet. A projection is made of the potential range of this type of system and it is suggested that detection of a tunnel such as the one studied at a 100 foot range is within theoretical limits.

DD FORM 1 JAN 73 1473 EDITION OF 1 NOV 65 IS OBSOLETE

UNCLASSIFIED

SECURITY CLASSIFICATION OF THIS PAGE *(When Data Entered)*

20.

The measurements were made at the Hazel A mine east of Gold Hill, Colorado in a real world terrain, i.e., on the side of a mountain over a rough ground surface. The tunnel itself does not have smooth walls but the relative positions of the radar and the tunnel could be readily determined.

The experiments were initiated by making propagation measurements from an antenna within the tunnel to one on the surface above the tunnel in order to fix the dielectric constant at $\varepsilon_r=6$. An attempt to find the conductivity in this manner was not successful.

The tunnel detection results were compared with theoretical estimates and found to be in reasonable agreement if the conductivity is assumed to be 0.002 mhos/m.

CONTENTS

INTRODUCTION

A series of experiments were made using the Video Pulse Radar System[1,2,3] at the Hazel A mine site east of Gold Hill, Colorado. The site and the tunnel depth were such that only the HFW radar[5] concept was applicable. Two trips were made to this site, one in August and one in October. The site is ideal in that the tunnel position could be accurately determined. It presented a realistic test in that the ground surface above the tunnel was in rough terrain located on the side of a mountain. A goal of the experiments was to evaluate the operation of the radar for the detection of tunnels. A second goal was to provide information that could be used to guide further development of the radar. Much was learned of the ways that improved data could be obtained in any future measurements. Based on the experimental data, a significant new approach was developed for processing the data. As we shall show we were also able to better pinpoint the limitations on detecting tunnels in this type of environment. Based on data and the theoretical results of References 5,6, we will suggest the limitations of such radar systems for tunnel detection in this type of media.

SITE INFORMATION

The following section summarizes the important data for the geometry of the Hazel A site. The features of the site are illustrated in Figure 1. The most important feature is that the tunnel is cut into the side of the mountain horizontally. Because of this a transit could be set near the entrance and a light source in the tunnel observed as a reference. By the use of the transit, we were then able to measure accurately the position of the radar antenna. As is indicated in Figure 1, measurements were made on rough ground in trees and large rocks. At times, the end of the extended HFW radar antenna was a foot off the ground. Other difficulties included holding the antennas in position as measurements were being made. There was at times a tendency for

LOCAL FEATURES IN THIS THIS TERRAIN INCLUDE:

1. TREES
2. ROCKS
3. ROUGH SURFACE GROUND — ROUGH TUNNEL WALLS
4. TUNNEL WIDTH 4' — 6'
   TUNNEL HEIGHT — { 6' FOR 10' DEPTH
                   { 10' FOR 20' DEPTH

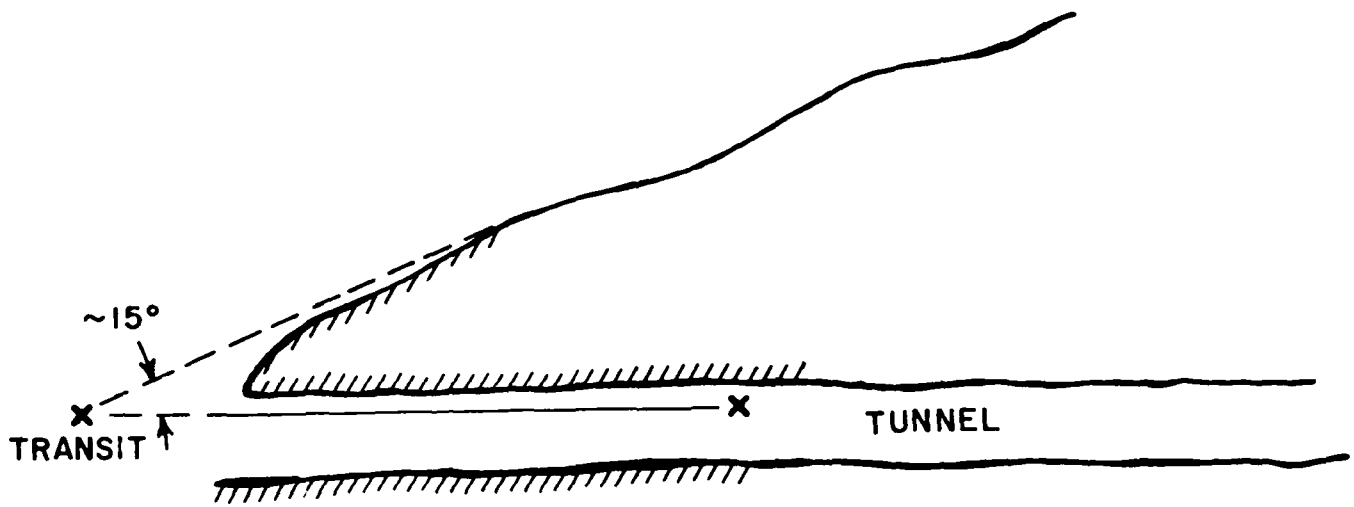

Figure 1. Sketch of tunnel geometry.

them to slide down the slope. Not only was the ground rough, but the tunnel walls themselves were rough with a scale height on the order of a foot.

Figure 2 shows the geometry of positions used in recording data for the shallowest site tested. The grid points represent the positions of the center of the antenna.

PROPAGATION MEASUREMENTS

Our initial measurements at the Hazel A site consisted of transmitting a pulse (6 ns) between an antenna mounted on the roof of the tunnel and one on the surface above. Because of the geometry, reasonably accurate position data were obtained for both antennas. This enabled us to evaluate the permittivity of the granite medium based on time of arrival data but we were unable to consistently evaluate the conductivity based on pulse amplitude. Figure 3 shows the received pulses for 10.1' and 18.8' propagation paths and indeed the time delay and decay of the pulses look appropriate. Figure 4, however, shows the decay for propagation paths of 35' and 38.3'. Now the signal over the longer path is almost double that of the shorter path. The time delay, however, is still consistent with the path differential. Figure 5 plots the time delays vs distance between antennas for a number of paths. A best fit straight line is shown connecting these data points. Based on these measurements, velocity of a wave in the media is 0.41 feet/ns and a relative permittivity is found to be 5.94, a value quite consistent for a granite media and in good agreement with values provided by Mr. Richard Myers of the Bureau of Mines.

Figure 6 shows a plot of the magnitude of the second peak of the received pulse as a function of range. Clearly no consistent results can be obtained from these amplitudes. Even more anomalous data was observed. For example at one location of a dipole inside the tunnel, the received signal directly above it was observed to be cross polarized.

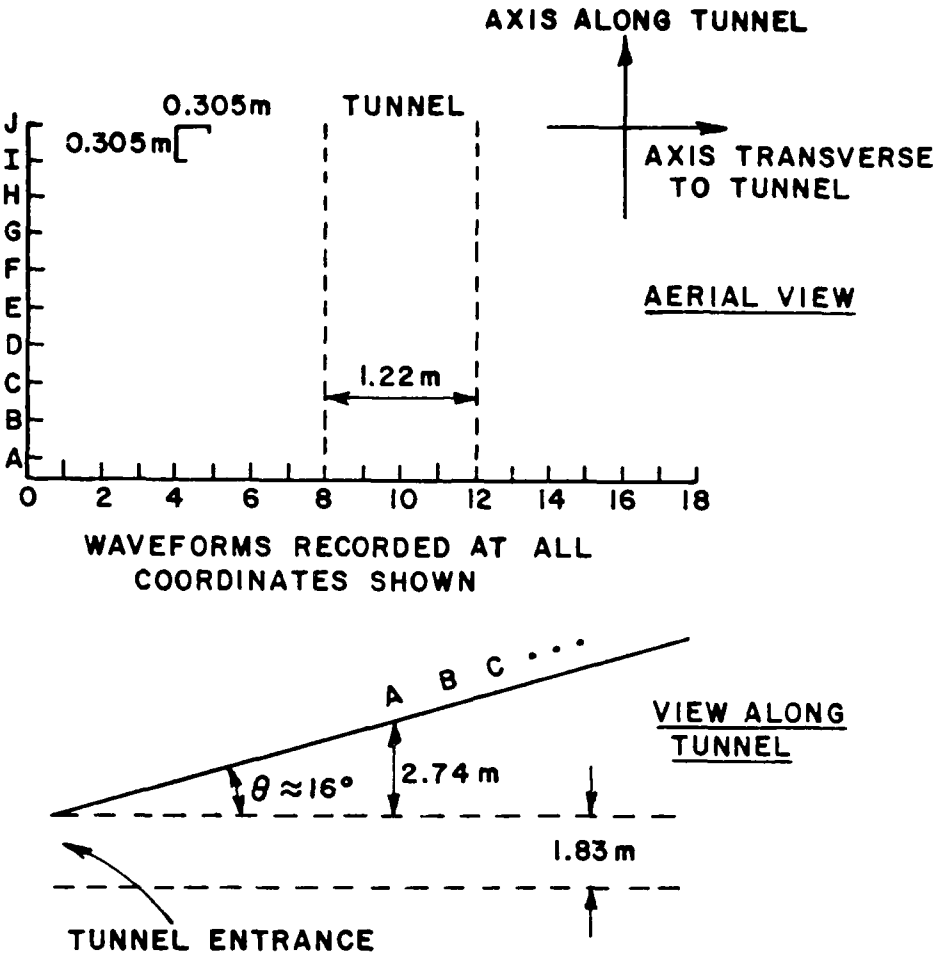

Figure 2. Map site and grid layout for shallow range.

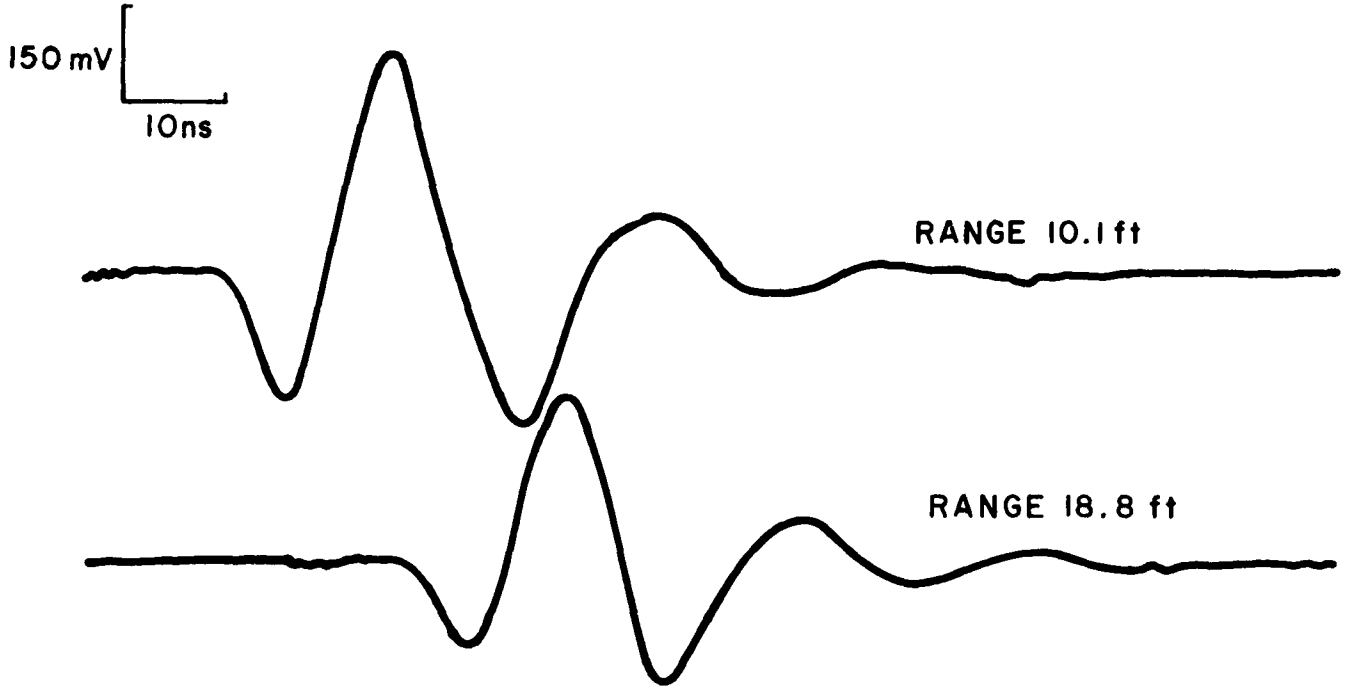

Figure 3. Waveforms transmitted from surface to antenna in tunnel.

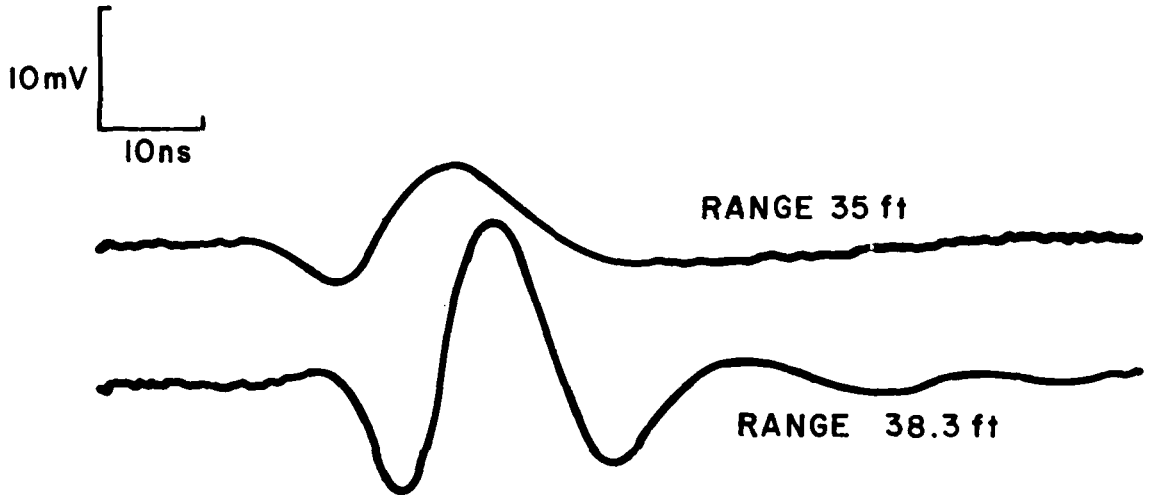

Figure 4. Waveforms transmitted from surface to antenna in tunnel.

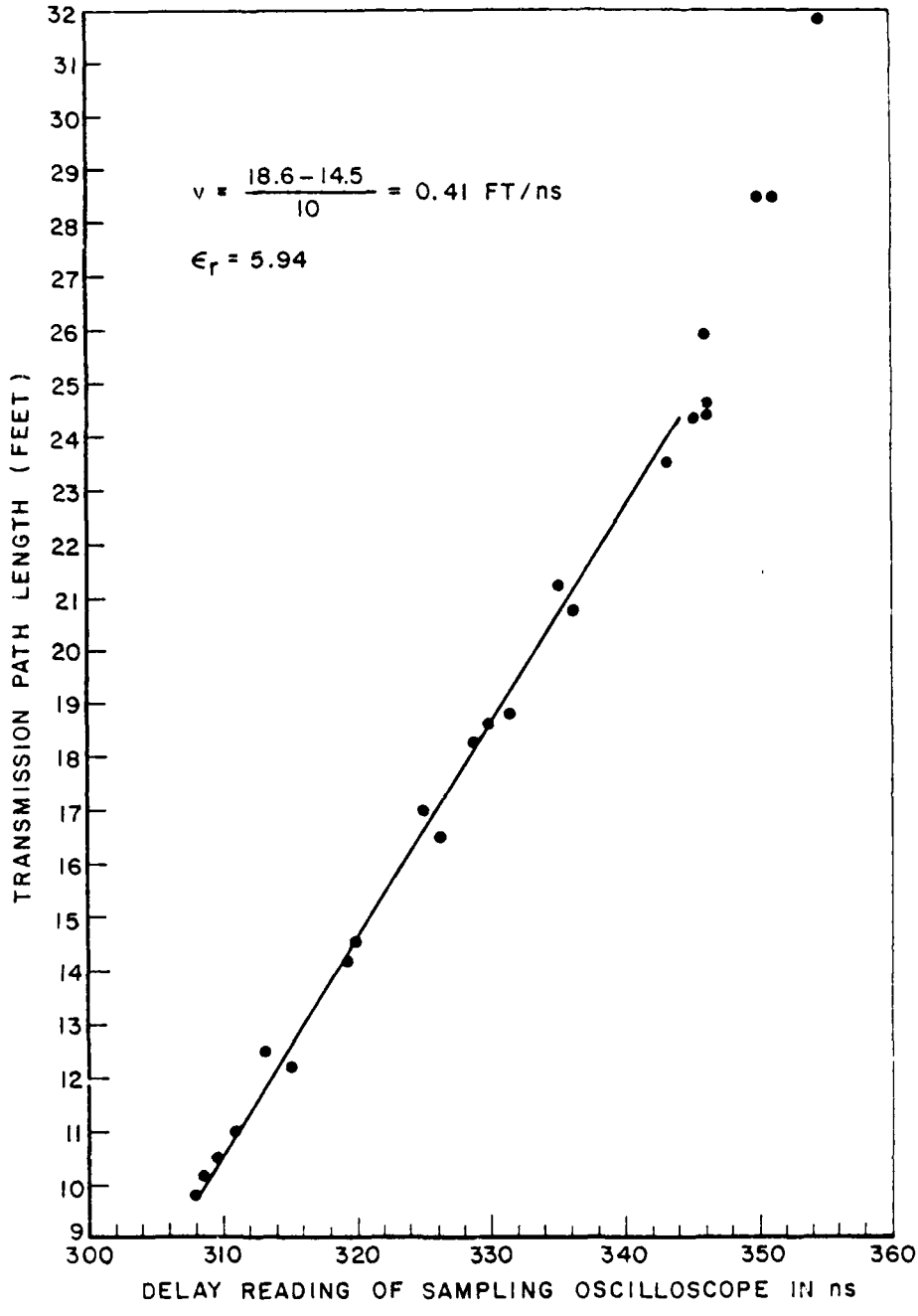

Figure 5. Measurement of time vs range from transmission between antennas on surface and in the tunnel.

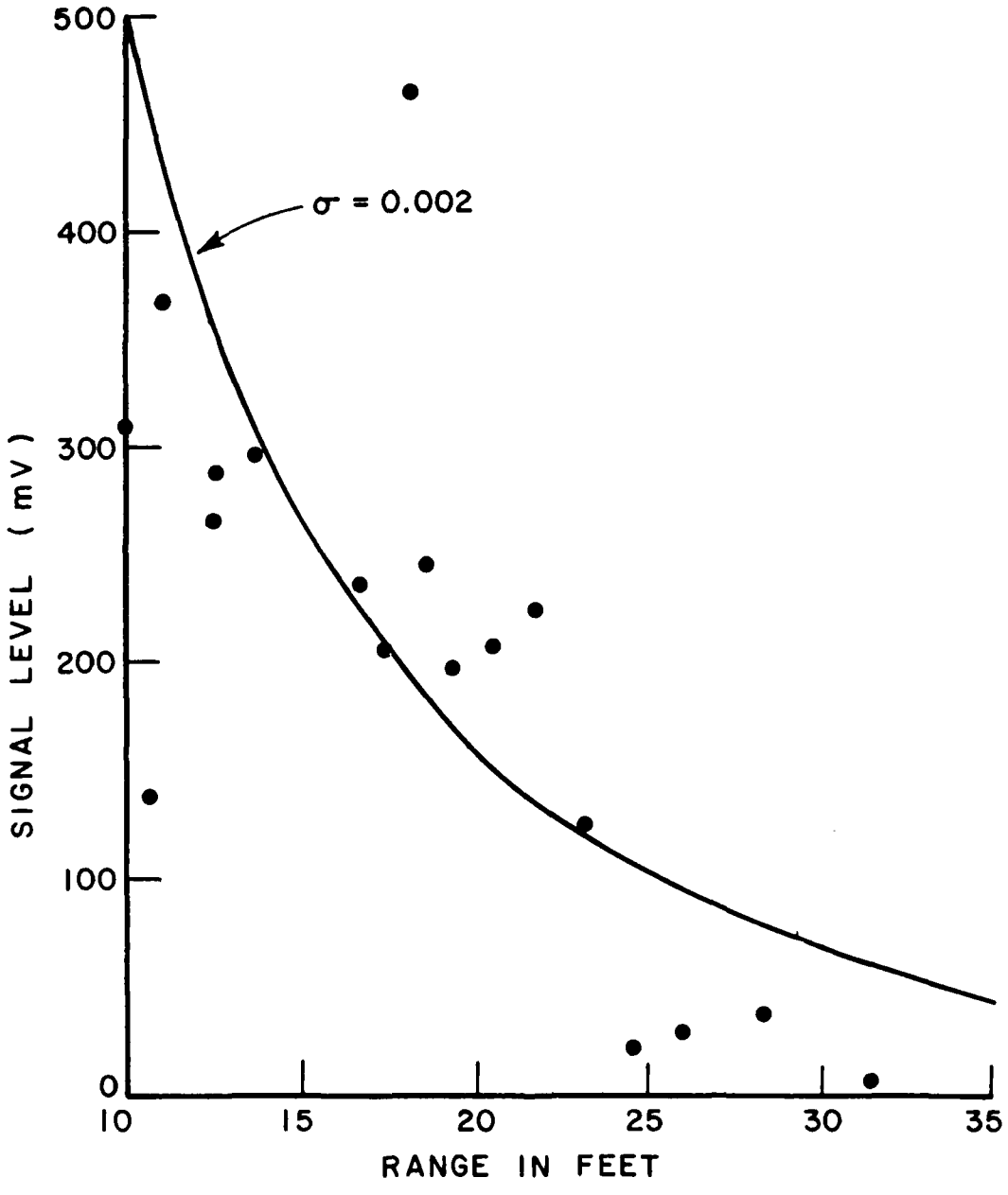

Figure 6. Level of 2nd peak of waveform transmitted between antennas on surface and in the tunnel.

Yet when the antenna was moved a few feet from directly above the tunnel, the received signal was polarized in the same sense as would be expected from the dipole in the tunnel. Similar behavior has been reported verbally to us by Bureau of Standards personnel.

SUMMARY OF RADAR MEASUREMENTS

The following radar scattering measurements have been made using the following systems:

1. The modified Terrascan antenna using a 6 ns pulser at positions where the tunnel roof was approximately 10 feet below the surface.

2. The Long Box Antenna (LBANT) at the above location.

3. The Long Box Antenna at a position when the tunnel roof was 20 feet below the surface.

4. The Long Balun Feed Dipole Antenna (LBFA) where the roof was approximately 43 feet below the surface and now using a step excitation with 15 ns rise time.

5. The Long Balun Feed Dipole Antenna where the roof was 55 feet below the surface.

6. The Long Balun Feed Dipole Antenna where the tunnel roof was approximately 73 feet below the surface.

Measurements 4, 5, and 6 will be discussed in a separate report[3].

RADAR PERFORMANCE FOR TUNNEL ROOF APPROXIMATELY 10 FEET BELOW SURFACE USING MODIFIED TERRASCAN ANTENNA

At this 10 foot depth, the expected time of arrival of the pulse scattered from the tunnel roof is 49 ns. The area above the tunnel was laid out in a rectangular grid 19 rows by 11 columns as has been shown in Figure 2. Each row was oriented transverse to the tunnel with waveform number 10 being at the position directly over the tunnel. The data are shown in Figure 7 for the third row (labeled c). Data in the other rows are similar in nature. These data were used to make the Grey Level Plot (GLP) shown in Figure 8. There were various processing schemes developed for making these plots. This is from one of the set given in Reference 7 which has a complete discusison of the grey level plots. The abscissa is the distance in feet in a path transverse to the tunnel. Position 10 is directly above the tunnel. The ordinate corresponds to the time scale of the waveforms of Figure 7 or depth into the ground. The expected tunnel depth is identified in Figure 8. At the appropriate depth and position, there is clearly a darkened area in this GLP. This reveals the presence of the tunnel even though it is very difficult to perceive in the raw data of Figure 7. The darkened regions above the tunnel represent the antenna clutter and ground surface clutter. The curvature in the shape of the darkened "tunnel" area is caused by the increased path length to the tunnel as the radar is moved away from the center position (10) on the surface. The radius of curvature of the darkened region approximately fits the computed value as given in Reference 7.

Figure 9 shows a grey level plot taken right over the tunnel moving up the mountain as the abscissa goes from A to J. Again the ordinate is a function of time or depth. We clearly see a darkened area moving from the tunnel location at A to the tunnel location at J.

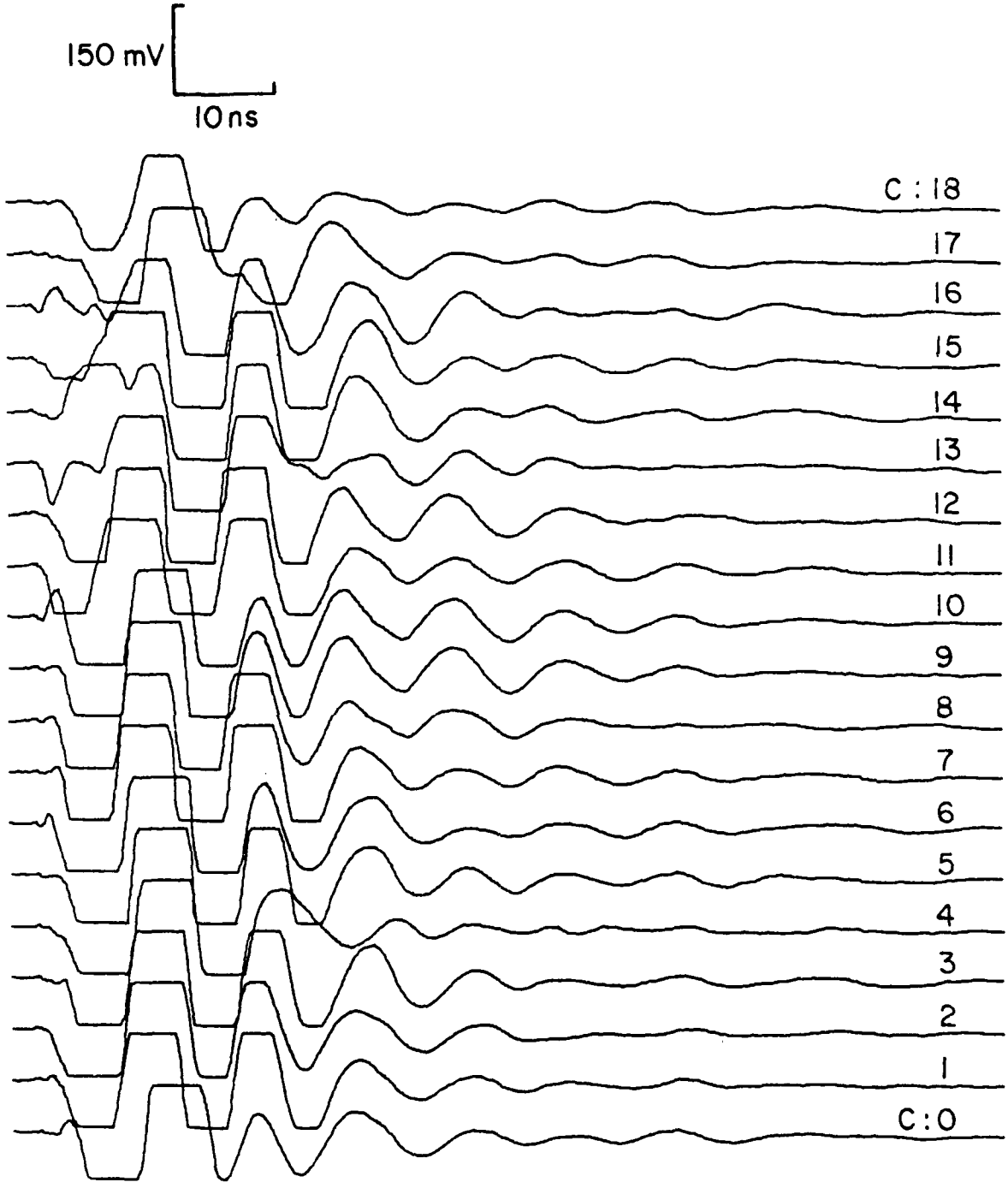

Figure 7. Radar waveforms for Terrascan antenna positioned over points in Row C.

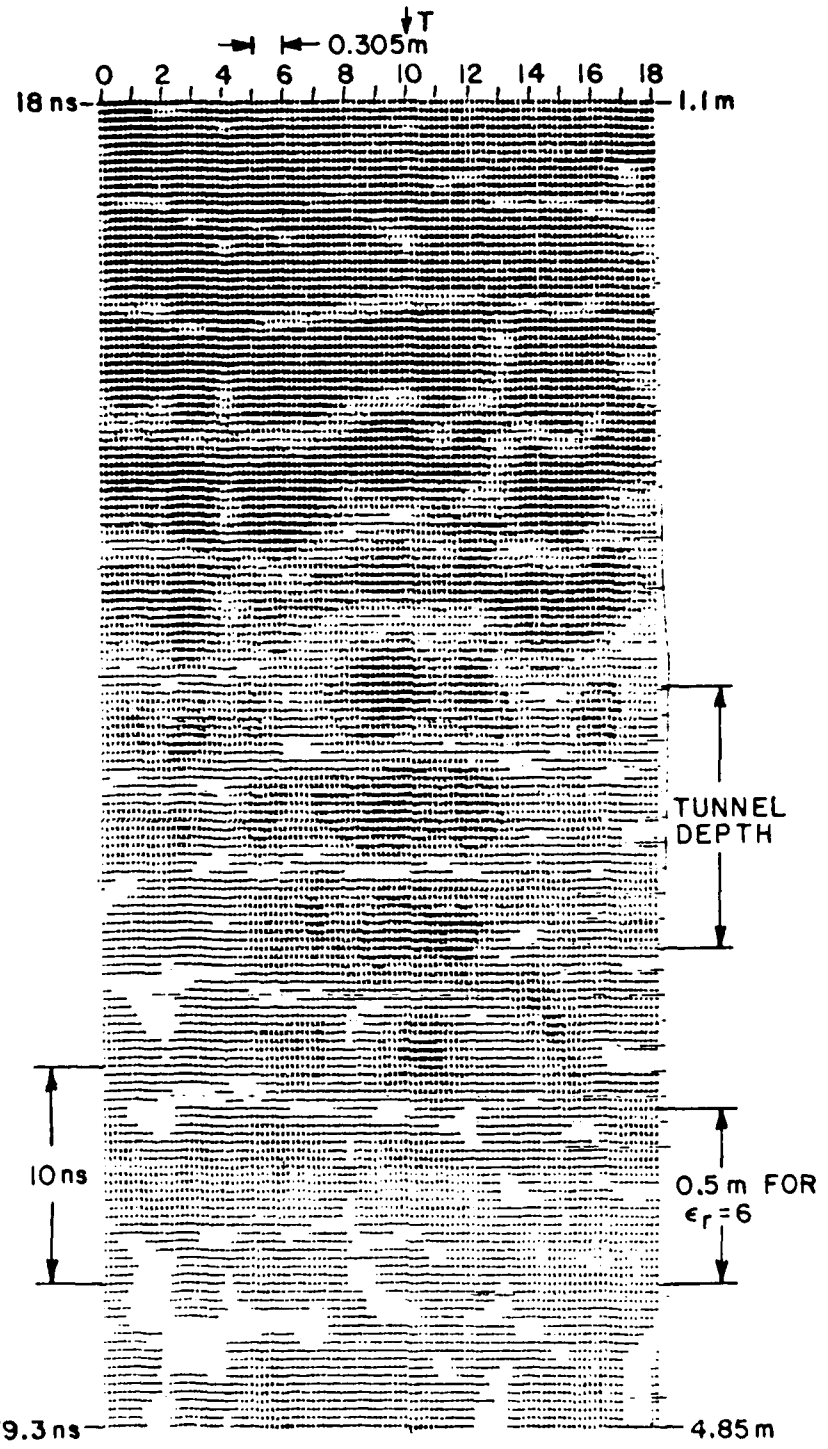

Figure 8. Grey level plot obtained from data of Figure 7.

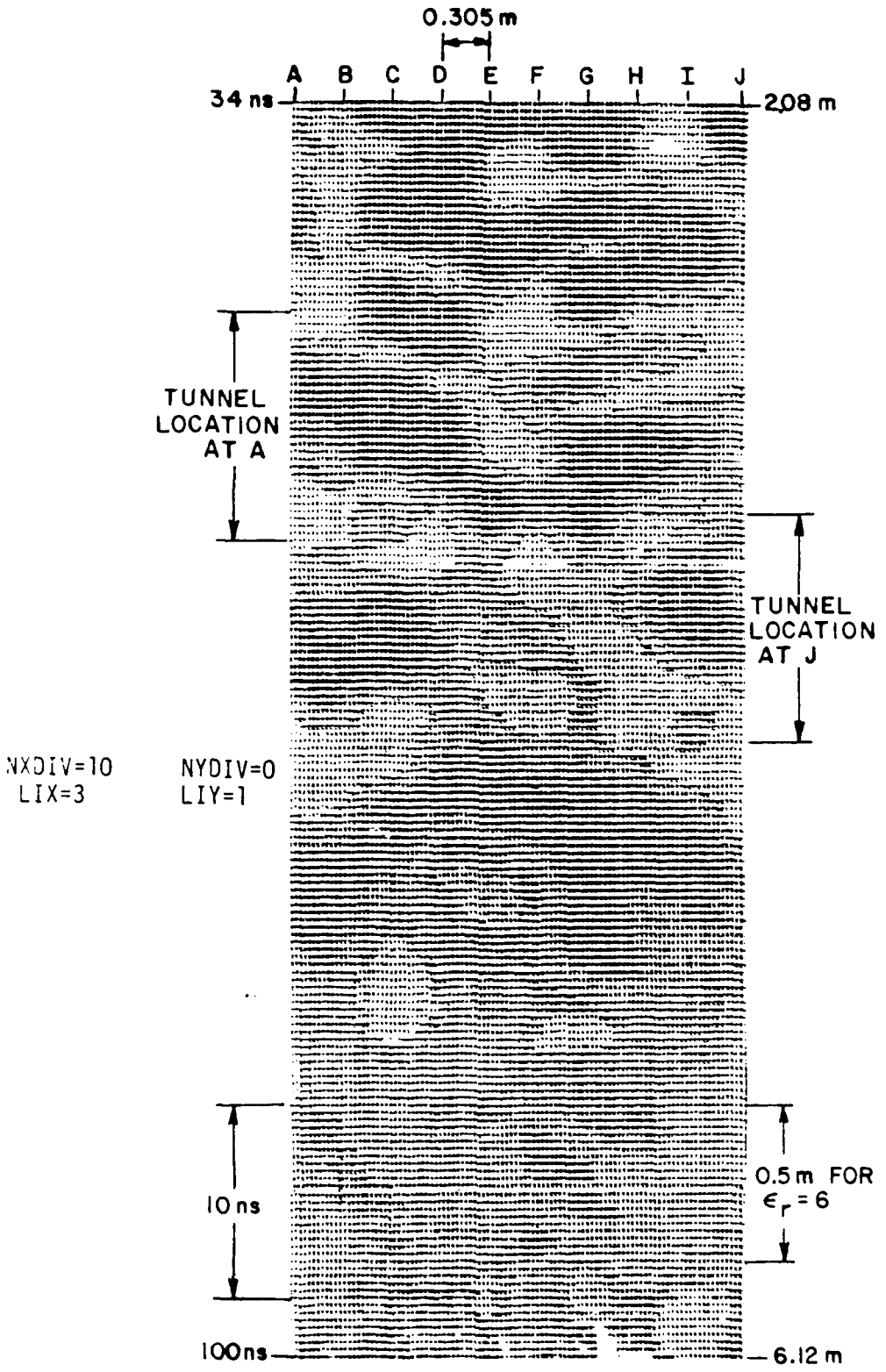

Figure 9. Grey level plot obtained when radar is positioned above tunnel (column 10) and moved from Row A to Row J.

DATA TAKEN FOR TUNNEL ROOF AT 10 FEET DEPTH USING
LONG BOX ANTENNA (LBANT)

The preceeding data was obtained using the modified Terrascan antenna[8]. This same data set was repeated using the Long Box Antenna[8]. The data set is shown in Figure 10 and the resulting GLP is given in Figure 11. Observe that the extent of the darkened area in Figure 11 is much greater than in Figure 8. This is probably because the antenna used was twice as long.

DATA TAKEN FOR TUNNEL ROOF AT 20 FOOT DEPTH USING
LONG BOX ANTENNA (LBANT)

The next data set was taken at a distance up the hill such that the roof of the tunnel was roughly 20 feet below the surface. The long box antenna and the 6 ns pulser were used to obtain experimental data over the sites illustrated in Figure 12. Waveforms are shown in Figure 13 and Figure 14 for the two sets of positions shown in Figure 12. The GLP is shown in Figure 15 for one of these paths. One sees a reasonable similarity between the GLP's of Figure 11 and Figure 15. Careful observation of the GLP of Figure 15 shows the darkened area near the tunnel seems to be centered at Q-8 instead of R-10. A reason given for this in Reference 7 is that at position R-10, the distance between tunnel roof and the surface is greater than for Q-8. This is because there is also a slope in the direction transverse to the tunnel as illustrated earlier in Figure 12b. This creates the type of geometry shown in Figure 16.

COMPARISON OF COMPUTED AND MEASURED RADAR RETURNS

Some recent computational results have been obtained for a 2 m square tunnel. Figure 17a shows the net cross-polarized Scattering Attenuation Function (SAF) of this square tunnel at a depth of 40 feet

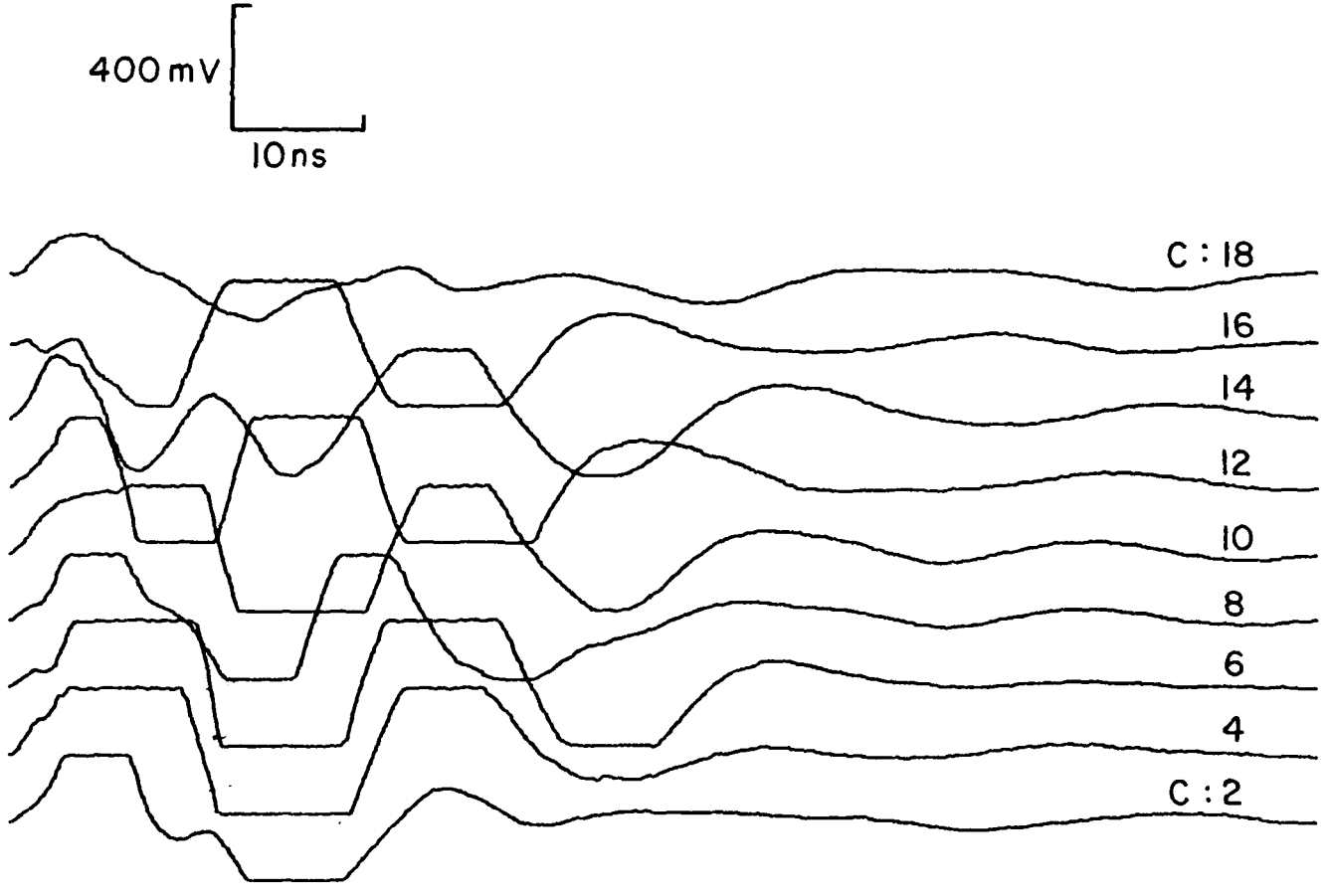

Figure 10. Radar waveforms for long box antenna positioned over points in Row C.

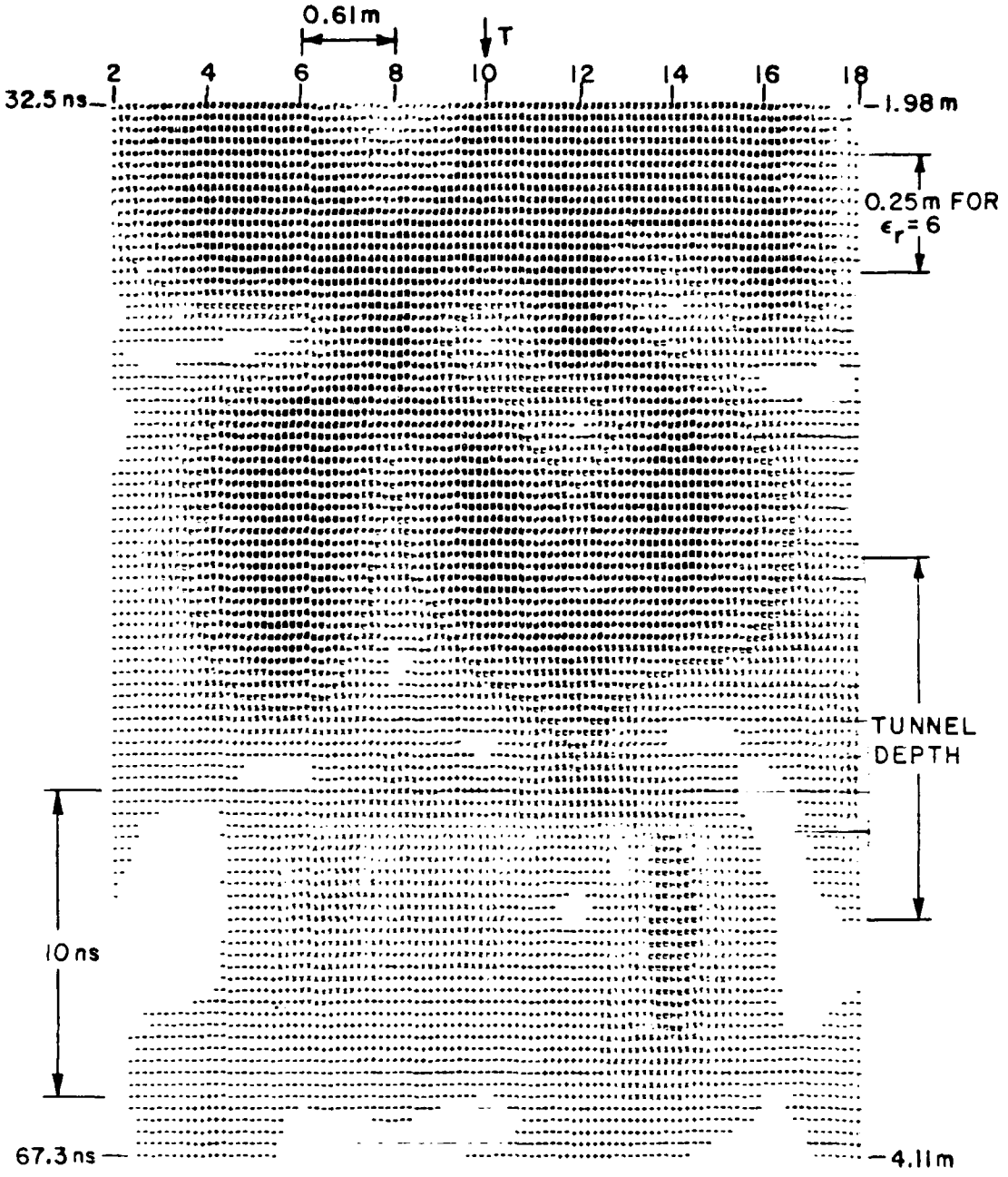

Figure 11. Grey level plot obtained from data of Figure 10.

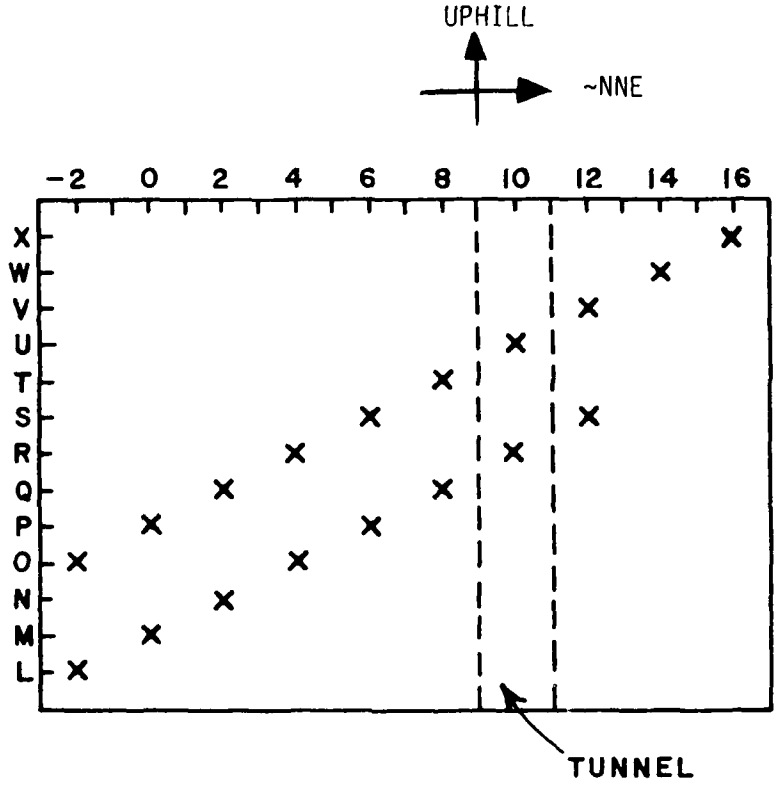

Figure 12a. Position for data at ~20 foot depth.

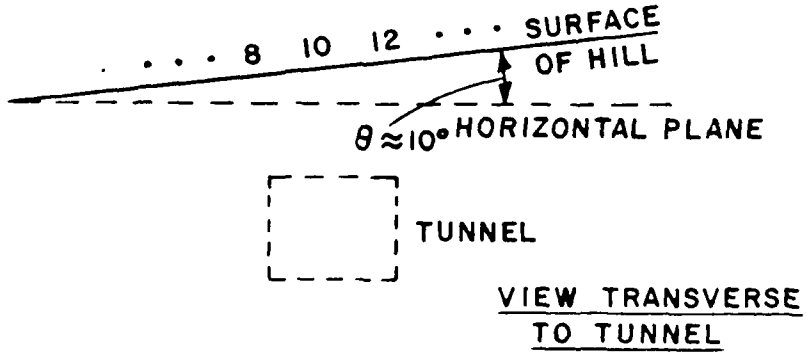

Figure 12b. Slope transverse to tunnel at ~ 20 foot depth.

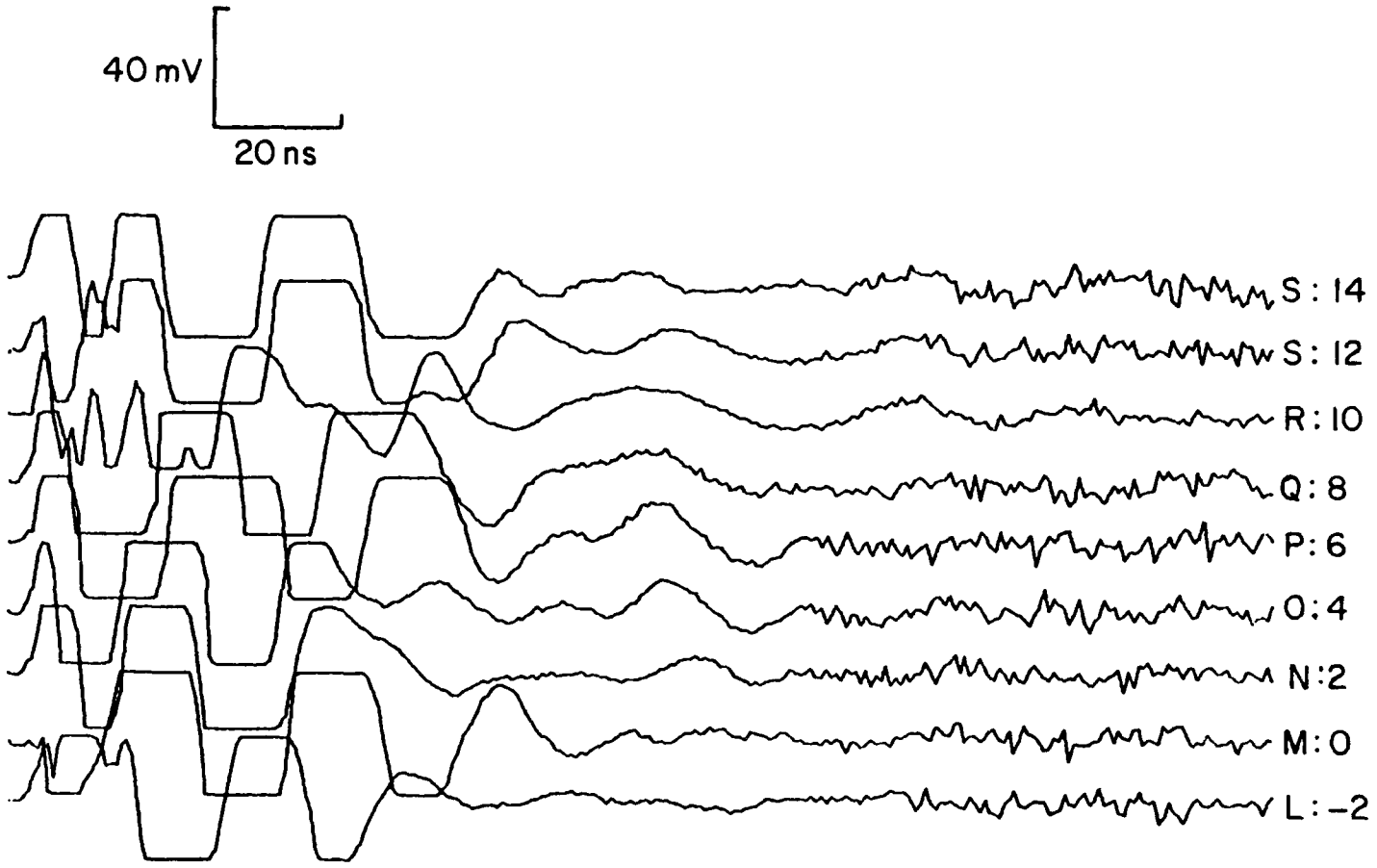

Figure 13. Waveforms recorded with radar along lower line in Figure 12.

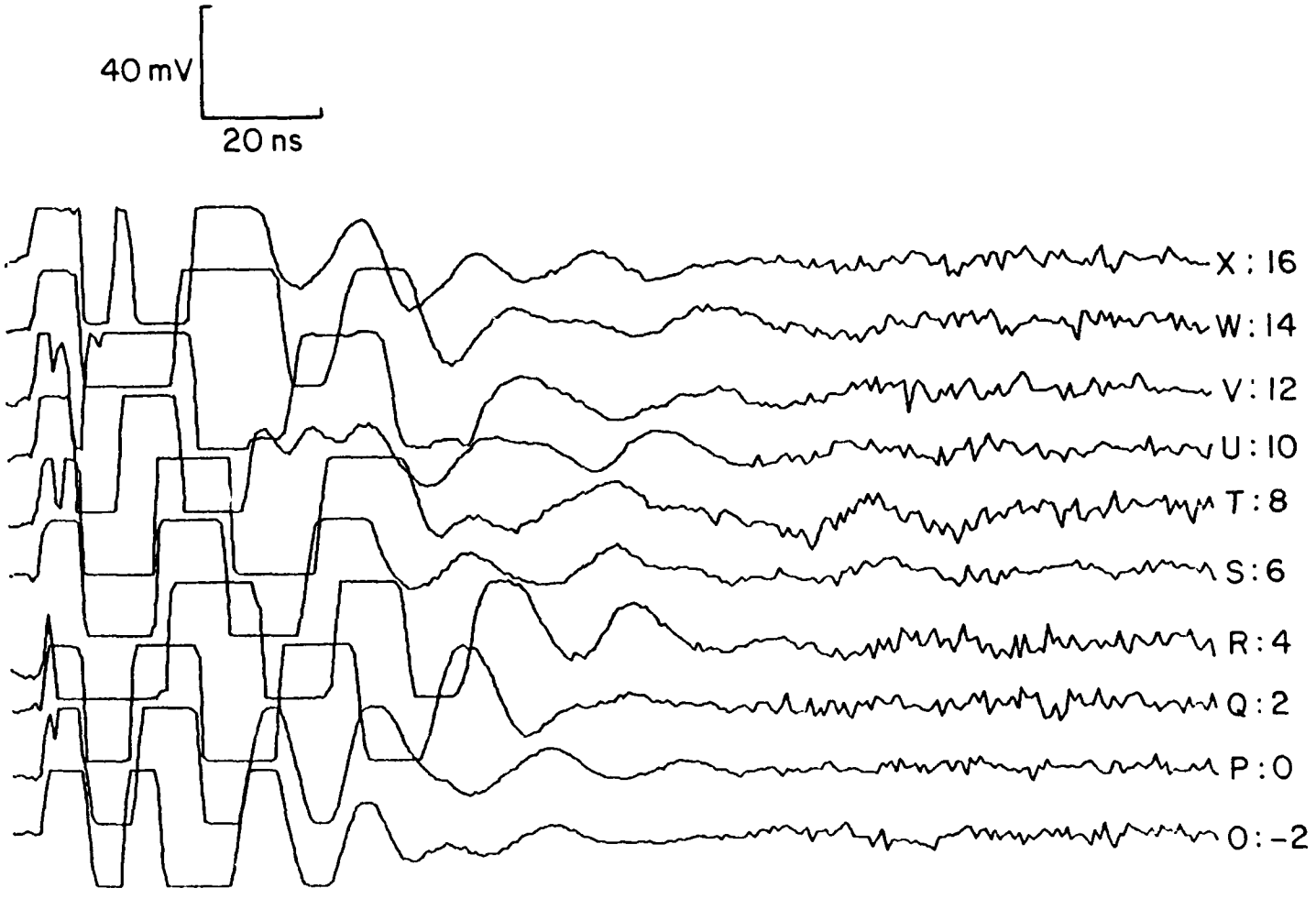

Figure 14. Waveforms recorded with radar along upper line in Figure 12.

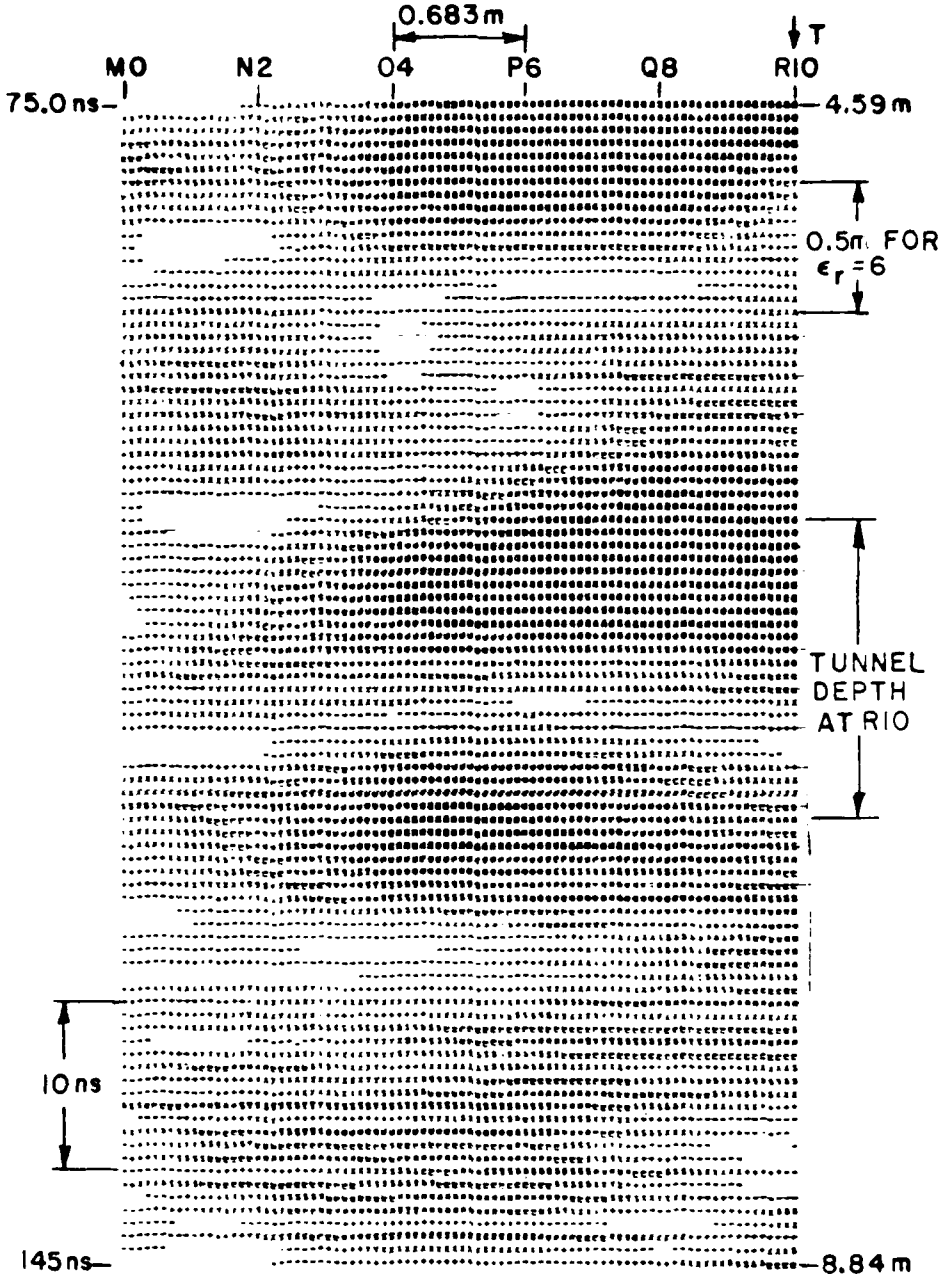

Figure 15. Grey level plot obtained from data of Figure 13.

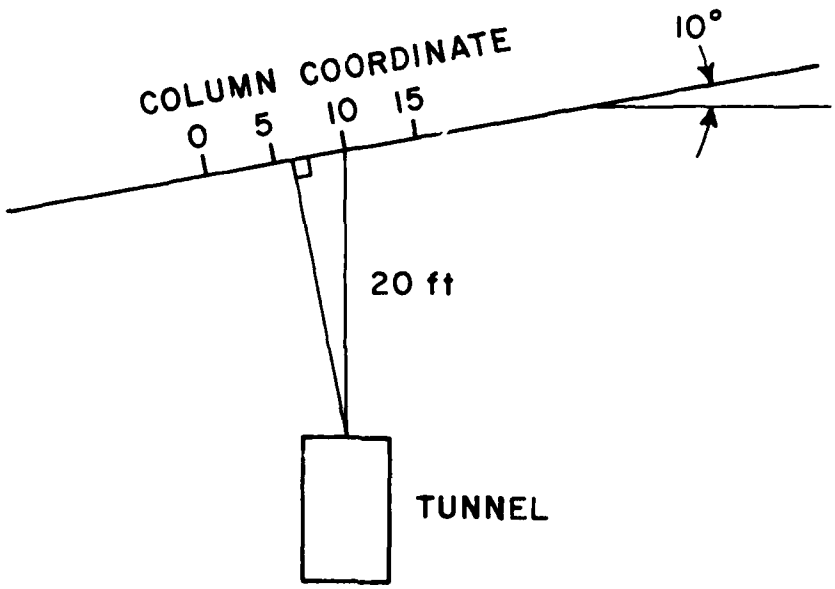

Figure 16. Illustration of nonhorizontal transverse geometry.

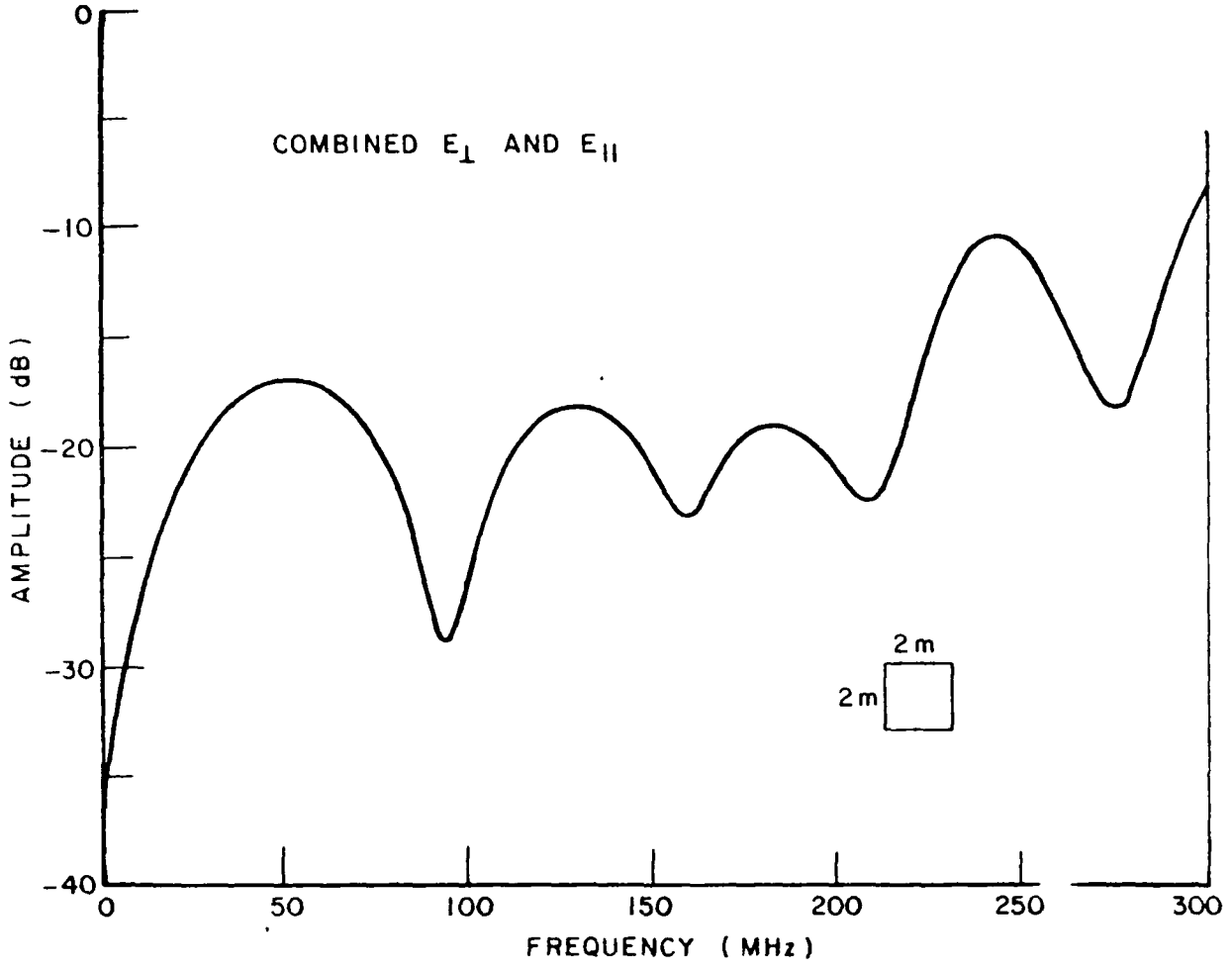

Figure 17a. Scattering attenuation function for a 2 m square tunnel immersed in a media with ϵ_r=4, σ=0.001 mhos/m at a 40 foot depth.

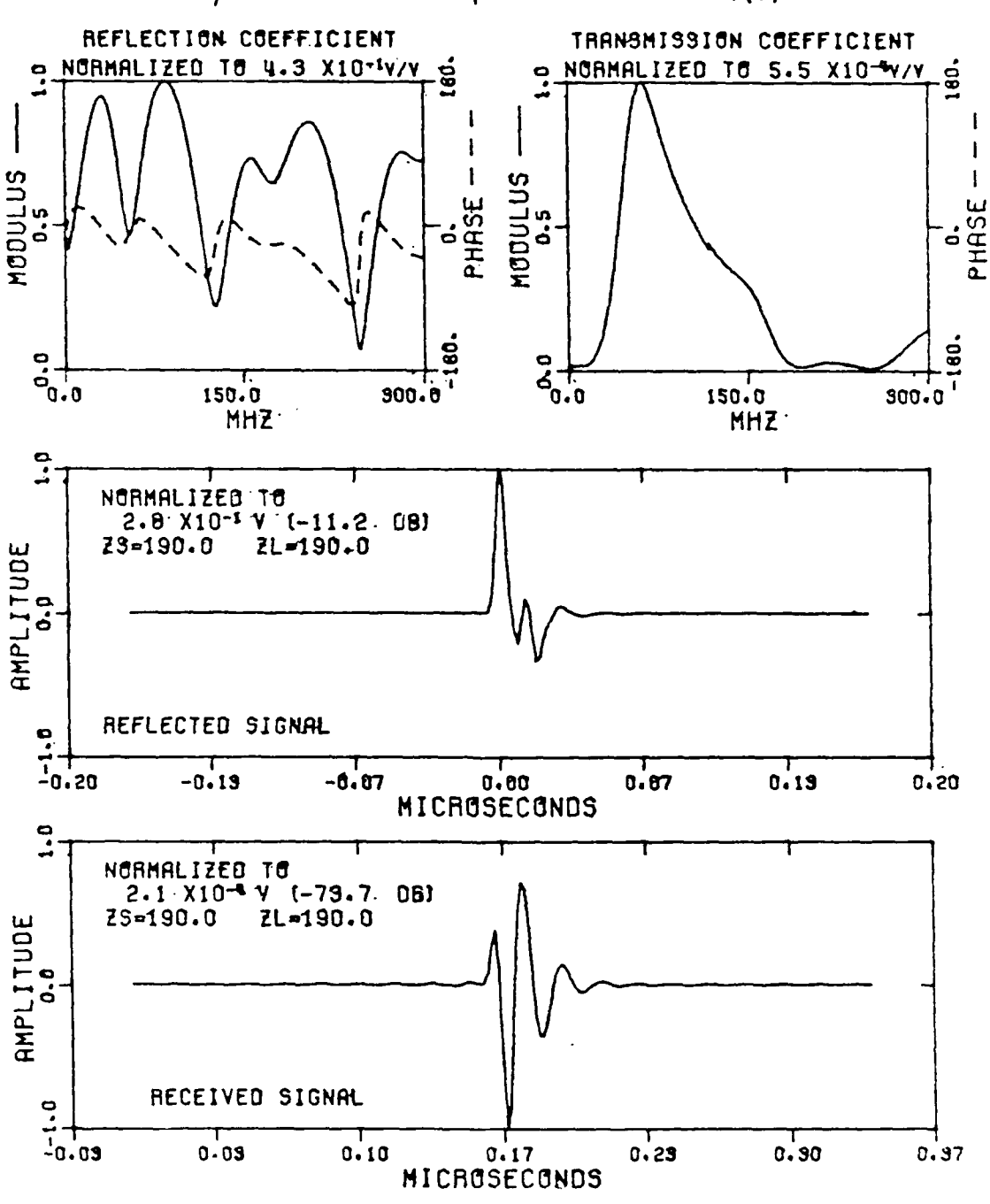

Figure 17b. Theoretical responses for propagation between two 4 foot long end loaded "Terrascan-like" antennas separated by 80 feet when excited by a 6 ns pulse. Folded dipole end load = 50 ohms, center load = 150 ohms.

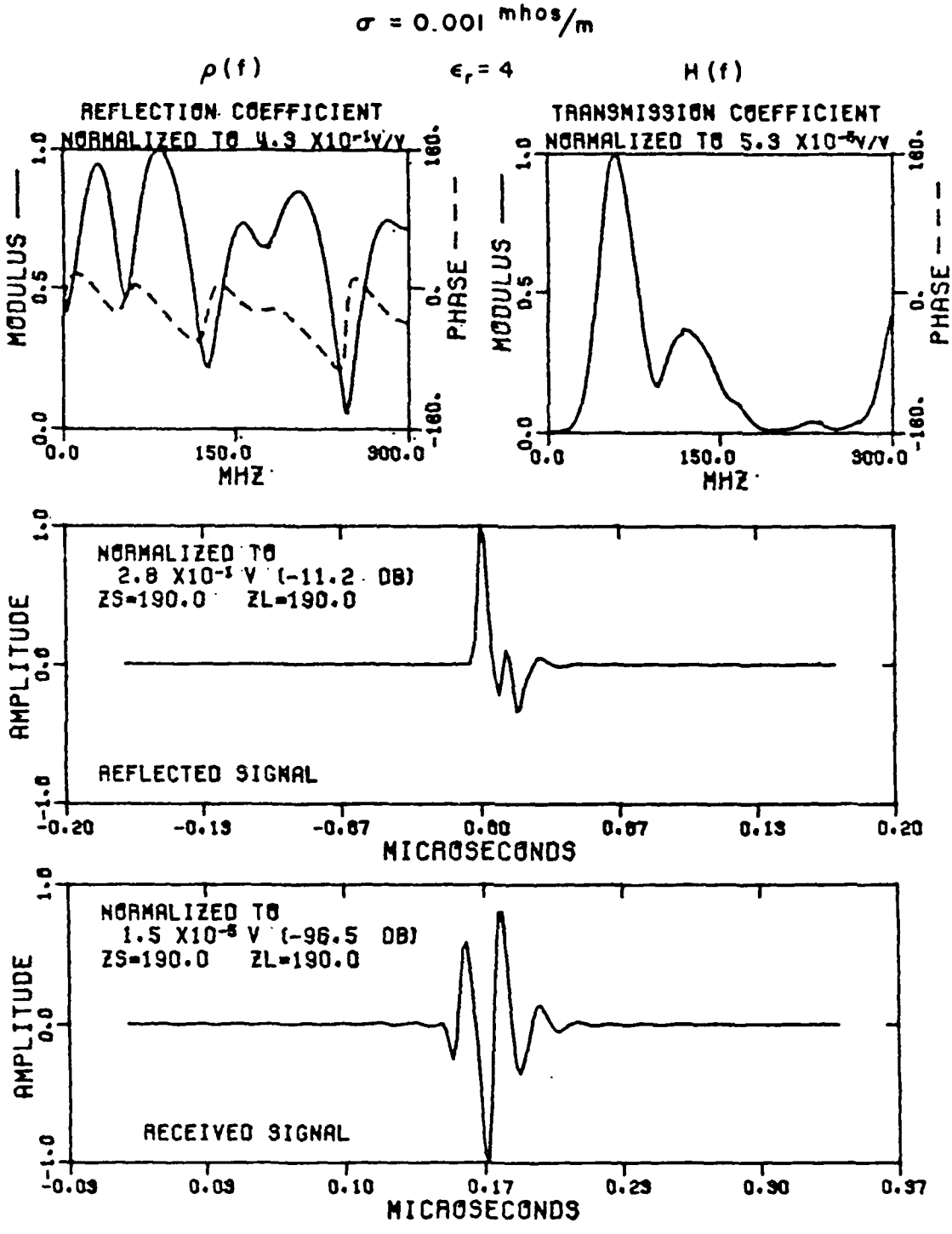

Figure 17c. Theoretical system response for 4 foot long crossed "Terrascan-like" antenna with end loading 40 feet above a 2 m square tunnel.

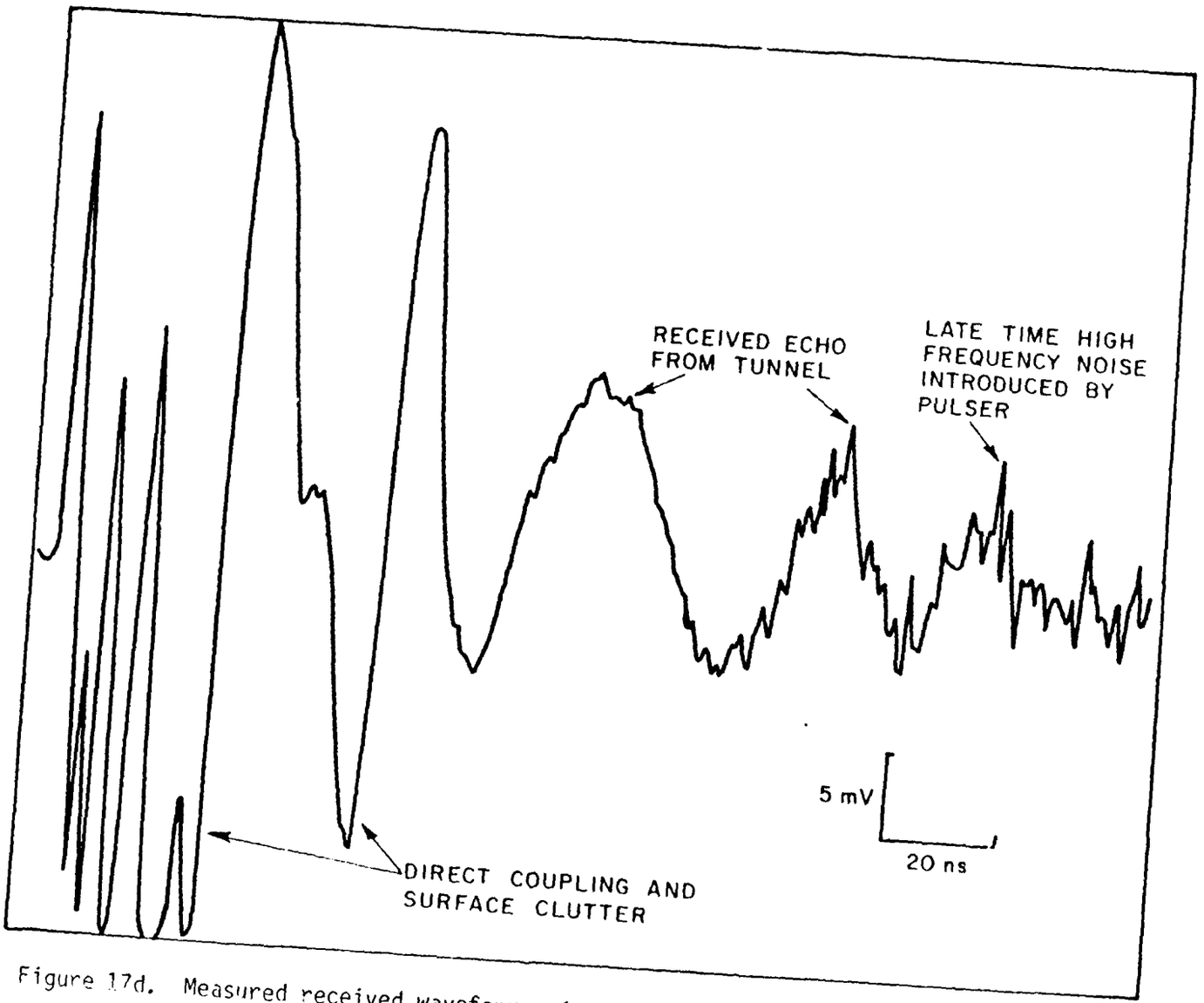

Figure 17d. Measured received waveform using LBANT antenna 20 foot above tunnel at Hazel A Mine Site east of Gold Hill, Colorado.

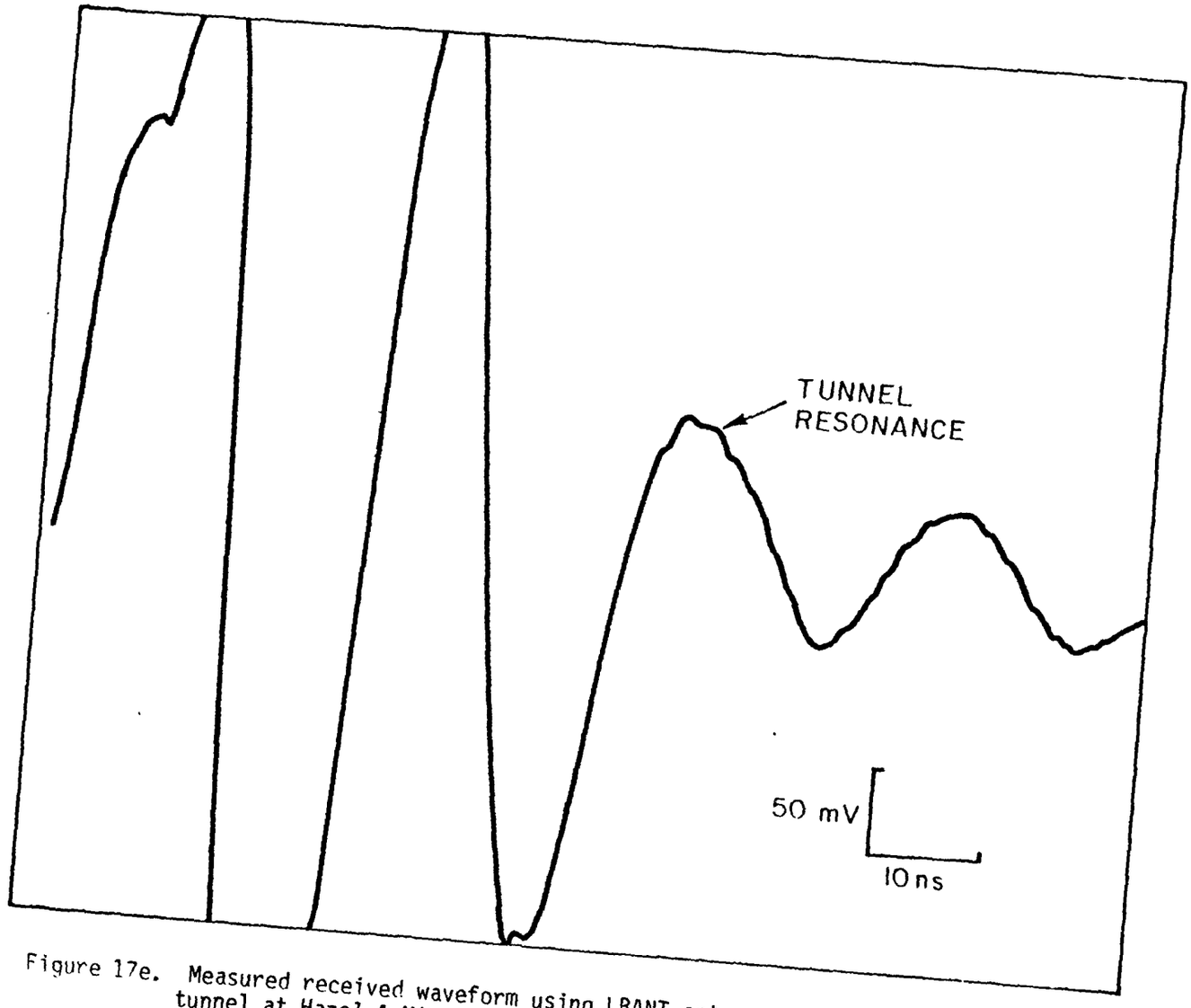

Figure 17e. Measured received waveform using LBANT antenna system 10 foot above tunnel at Hazel A Mine Site east of Gold Hill, Colorado.

in a medium with ε_r=4 and σ=0.001 mhos/m. The cross-polarized SAF contains the effect of both parallel and perpendicular polarizations. In Reference 1, it is shown that the SAF nulls for the parallel polarization are strongly suppressed at low frequencies and that there is a shift in position of the nulls between parallel and perpendicular polarizations. This might be anticipated if the tunnel is modeled by a waveguide structure. It would be further anticipated that a narrower tunnel (e.g., the 4 foot wide tunnel at the Hazel A site), would produce even larger differences in null positions between polarizations, and the level of Figure 17a would be increased.

Theoretical responses have been obtained for an approximate model of the BANT antenna (half as long at the LBANT) over a tunnel at a 40' depth for ε_r=4, σ=0.001 to be used in conjunction with the SAF just discussed. The antenna model is a modified version of the Terrascan system with end loading included. The analysis basically used the same model developed by Tribuzi[9]. The received waveform without the SAF is shown in Figure 17b for a 6 ns pulser excitation. Figure 17c shows the responses when the SAF is included.

In the following discussion, an attempt will be made to fit the data measured to the computed values using techniques outlined in Reference 5. It is important to realize that there are enough unknown parameters to make this a hazardous task. At best, it might be useful in fixing some of the unknown parameters. However, it is also important to determine if the measured signals are at least realistic.

Figure 17d shows the received tunnel waveform when the antenna position is approximately 20 ft above the roof of the tunnel using the 6 ns pulser and the LBANT antenna. At this position the dimensions of the tunnel were approximately 4'x9'. Several of the received voltage waveform parameters can be obtained from Figure 17d. First and most obvious is that the peak value of the receive target signal is about 9 mv.

In order to allow reasonable comparison between measured and computed radar returns, certain features in the experimental system which are not included in the computational model must be removed. An experiment was performed which routed the 6 ns pulse through the radar system's 160 foot delay cables and both balun transformers (features not included in the computational model). The resulting effective pulse amplitude for comparison purposes was found to be 134 volts. This places the 9 mv return at -83.5 dB below the transmitted signal.

The computed value obtained for a 2 m square tunnel with the Terrascan antenna for a depth to the tunnel center of 40 foot was -96.5 dB (with ε_r=4, σ=0.001). We now will show these two sets of data are consistent provided the conductivity at the Hazel A mine is σ=0.002 mhos/m, (ε_r=6 is well established).

Considering the computed results, from the curve of Figure 26 of Reference 5 the medium attenuation function A_F ~ 41 dB. From Table 2,[5] the constant A_1=32.9 dB for a one meter long antenna. The propagation computation of Figure 17b gives the sum as 73.7 dB showing that these estimates are reliable. From Figure 17b and Figure 17c we obtain the SAF for this geometry as 23 dB. The value of A_F is the principle term dependent on the depth and the electrical parameters. Also recall that the computation is based on a tunnel whose center is at a 40' depth. The tunnel roof for the measured data is at a depth of 20 feet. Correspondingly the center is adjusted to a depth of 23 feet and the resulting value of A_F for the ε_r=4, σ=0.001 medium is -27 dB.

This is adjusted to -34 dB for the ε_r=6 and σ=0.002 mhos/m medium. Using the rules of thumb set up earlier[6] we can adjust the computed signal level to the one that would be anticipated for this present case.

1. The change in ε_r from 4 to 6 yields a decrease in SAF of 2 dB.

2. The change in conductivity from 0.001 to 0.002 mhos/m increases the SAF by 3 dB.

3. The change in depth from 40' to 20' increases the SAF by 3 dB. This yields a net increase in the scattering attenuation function of 4 dB. Doubling the antenna length to conform to the antenna size used in the experiment increases the received signal by about 6 dB resulting in a computed net value for the final geometry of -80 dB.

From Figure 17d one can also estimate the frequency of the signal returned from the tunnel. One period of this waveform ranges from 30 to 40 ns and the corresponding frequency ranges from 25 to 33 MHz. From Figure 17a, it is observed that the first resonance in the 2 m square tunnel is at 50 MHz; however the height of the actual tunnel had increased to about 3 m for this particular position (the width was only 4'). This would decrease the resonant frequency to about 33 MHz. With all the clutter present to disturb the waveforms, this is seen to be within the expected range. Since the permittivity is well established at 6.0, the expected arrival time for this tunnel 20 ft deep (to the roof) is approximately 100 ns. The measured arrival time of the first peak in the tunnel response is at approximately 90 ns. This agreement is again reasonable. Thus we see that this measured waveform does indeed conform to expected values and that we are indeed observing the tunnel.

Figure 17e shows the received signal level when the roof of the tunnel is approximately 10 ft below the surface. At this point, the tunnel height is reduced to about 2 m. The first and most obvious feature of Figure 17e is that the frequency content in the later portion of this waveform is approximately 45 MHz and indeed agrees well with the computed resonant frequency of the 2 m square tunnel. The magnitude of this peak associated with the tunnel is now approximately 60 mv or is approximately 67 dB below the transmitted signal. The attenuation factor is changed from 34 dB to 20 dB by this additional decrease

in depth and the SAF is increased by 3 dB giving a total increase in signal level of 17 dB. The computed signal level is now 63 dB and again agrees well with the measured value of 67 dB. The observed time of arrival of this signal is of the order of 55 ns in contrast to a computed time of arrival of 50 ns.

INTRODUCTION TC NEW POLE REMOVAL PROCESS

Even though the data given in Figures 13 and 14 is corrupted by clutter of various categories, a reasonably good map was obtained. However, the data can be processed in such a way that a much improved map can be generated. This was done and a number of modifications in the grey level plotting routine have been discussed[7]. However we have also been developing a new uniform processor under Contract N00014-78-C-0049 that appears to be a major breakthrough. This is a further development of some of the target identification concepts being pursued so successfully for the identification of "mine like" targets under Contract DAAK-70-77-C-0114. The goal of this process is to reduce the clutter in the waveforms by emphasizing the natural resonance of the tunnel in these time domain signals.

The first step in this process is to identify all of the poles in each received waveform by means of the Prony procedure. This basically uses techniques that have been pursued for buried targets under Contract DAAK-70-77-C-0114.

To remove any poles associated with one of the measured waveforms we introduce a difference equation:

$$R_{i-1}(nT) = -2\, R_e(Z_d) R_i(nT-T) + |Z_d|^2\, R_i(nT-2T) \qquad (1)$$

where $R_{i-1}(nT)$ = sample of waveform at t=nT with i^{th} pole removed

$R_i(nT-T)$, $R_i(nT-2T)$ = samples of waveform from which the pole is being extracted

$Z_d = Z_R + jZ_m$ = is the complex pole being removed (in the z domain), and

T = sampling interval

Observe that

$$Z_R = e^{\sigma T} \cos \omega T \text{ and}$$

$$Z_m = e^{\sigma T} \sin \omega T$$

where

$s = \sigma + j\omega$ = complex frequency.

To extract the antenna pole, values obtained from Equation (1) are simply added to the measured waveform on a point by point basis. This process is then simply "marched" through the measured waveform. A sampling interval is set equal to 10 ns. Thus a time to initiate the process is selected. Then a point is extracted from the measured waveform at a time 20 ns later. A new initial point is then selected (in this case, the time between samples of the sampling oscilloscope or (200 ns)/(256 points)) and the process is repeated. The resulting waveform is next passed through a band pass filter with a passband in the region between 10 and 120 MHz. The result is shown in Figure 18.

Now in the waveform after the antenna pole extraction process and filtering, we assume only the pole introduced by the tunnel scattering remains. Thus the waveform with the antenna pole extracted can now be rewritten in the form of a difference equation

$$|Z_d|^2 R_{i-1}(nT-2T) = - [R_{i-1}(nT) - 2 \mathrm{Re}(Z_d) R_{i-1}(nT-T)] \qquad (2)$$

Observe that the sign of Equation (2) differs from that of Equation (1). Now consider the terms on the right hand side of Equation (2) as being obtained from the R_{i-1} waveform at t=nT, nT-T. Then the term on the left hand side $R_{i-1}(nT-2T)$ is the predicted value $R_p(nT-2T)$. We obtain

$$|Z_d|^2 R_p(nT-2T) = -[R_{i-1}(nT) - 2 \mathrm{Re}(Z_d) R_{i-1}(nT-T)] \qquad (3)$$

We now observe that this predicted value of the waveform has been obtained by marching backwards in time.

APPLICATION OF POLE REMOVAL PROCESS FROM GOLD HILL DATA

The technique just discussed removed the antenna pole with time marching in the forward direction. However in almost all of the waveforms of interest, the early maxima have been clipped. This is a result of setting the receiver sensitivity high enough to see the target which causes system saturation of the early time response. This leads to errors in the pole removal process. Thus the decision was made to start with the late portion of the waveform and work toward early times. This involved changes in the detail but not in the concepts.

The results shown in Figures 18a-18h are obtained from the measured waveforms of Figure 13. First, the poles are determined for each waveform of Figure 13. Next, the pole associated with the antenna is extracted using the process described. If we had started with the early time and marched forward, using these clipped waveforms would cause errors to be introduced in the early part of the tunnel response. This produces the solid curve in Figure 18. Now we apply Equation (2) starting with the late time response. This results in the broken curve.

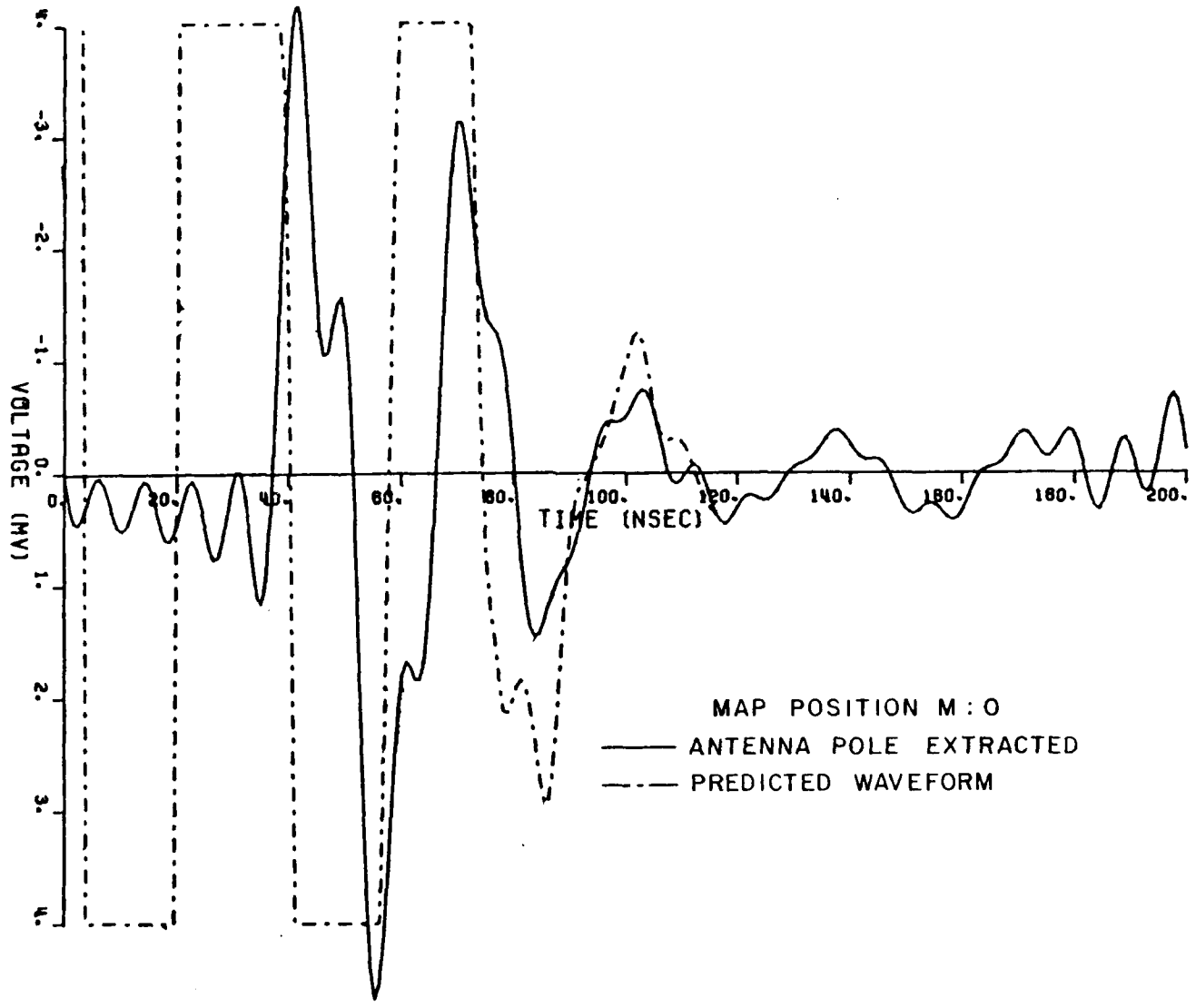

Figure 18a. Processed waveforms from experimental data 20 foot above tunnel at Hazel a Mine Site.

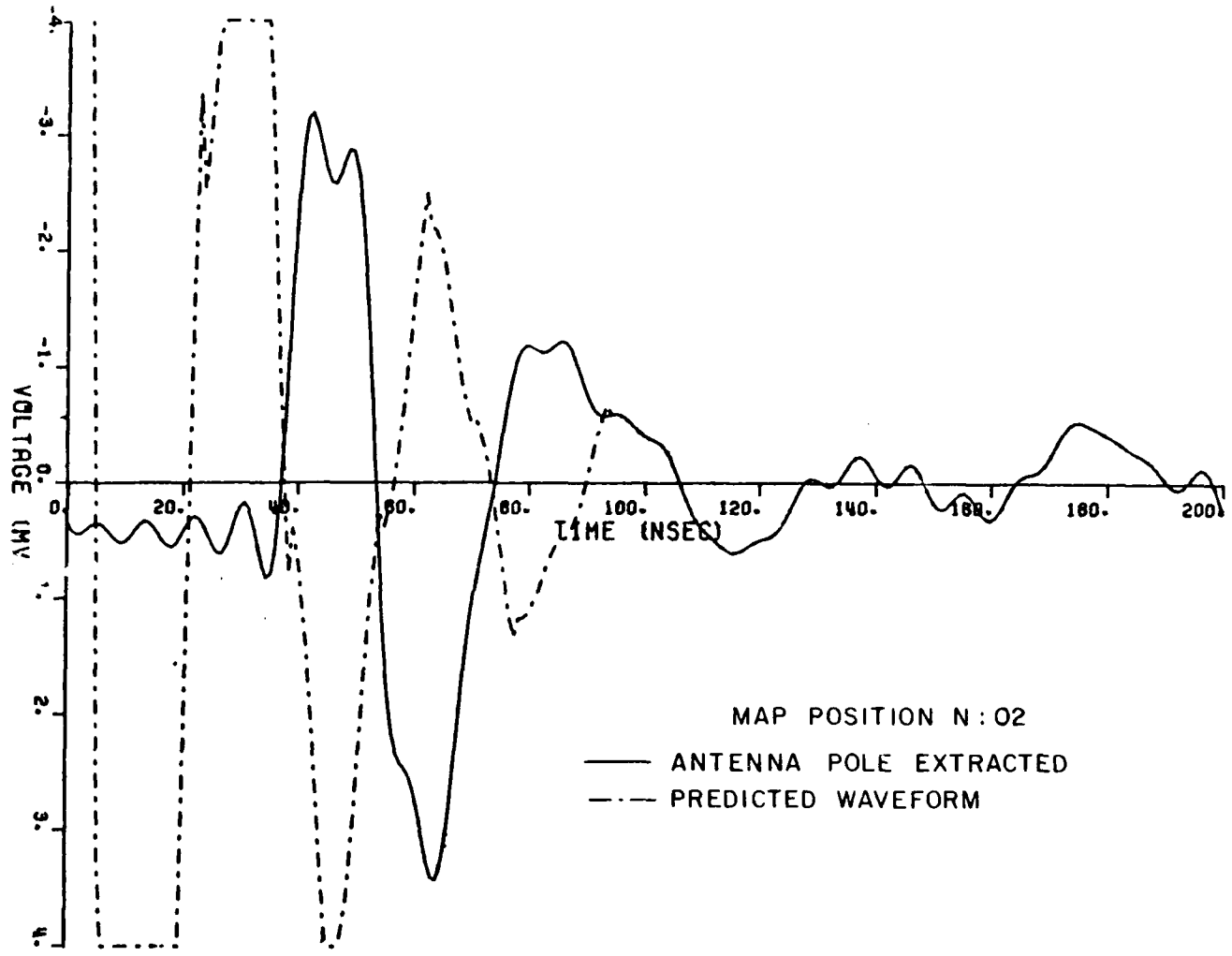
VOLTAGE (MV
TIME (NSEC)
MAP POSITION N : 02
ANTENNA POLE EXTRACTED
PREDICTED WAVEFORM

Figure 18b.

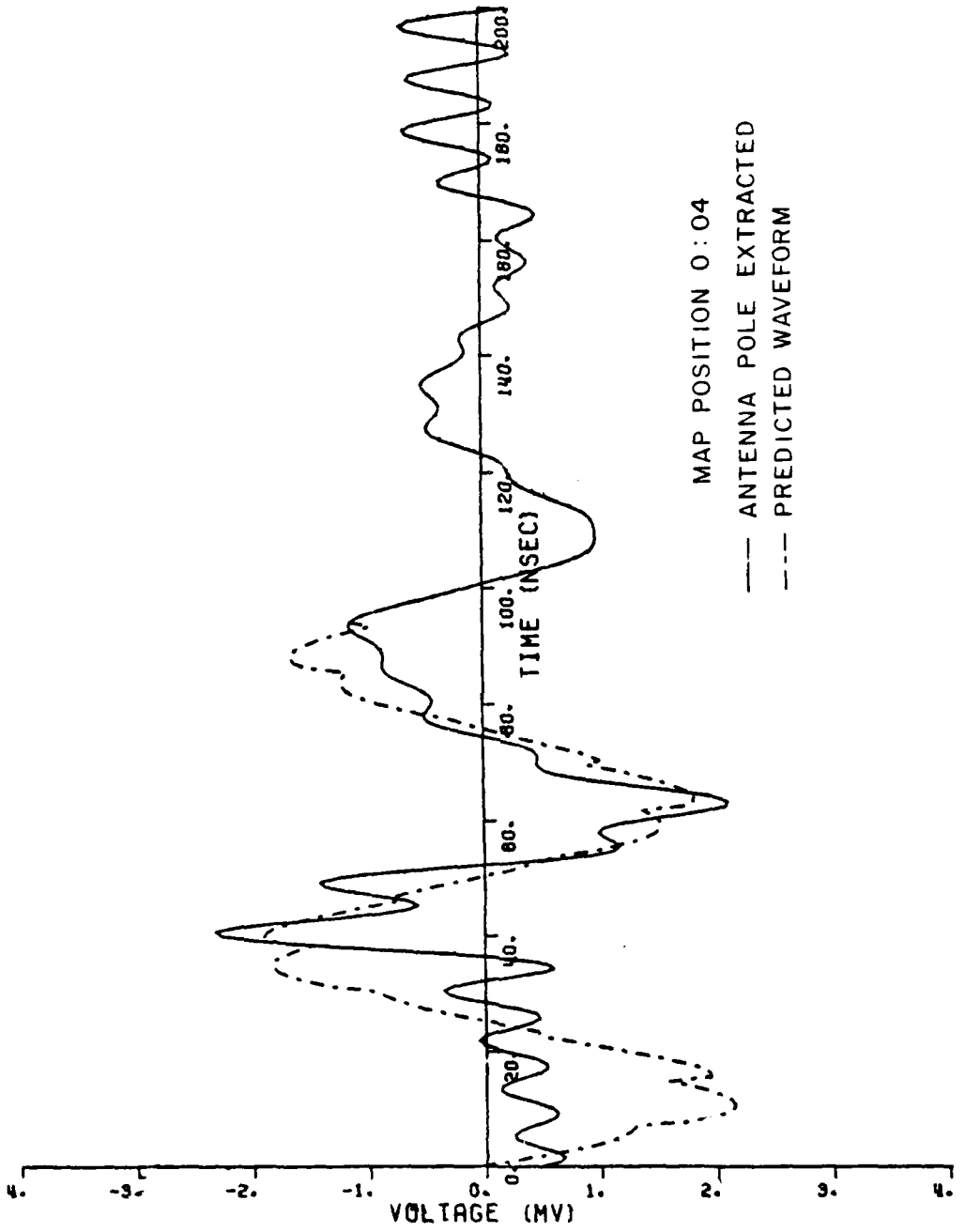
MAP POSITION 0:04
ANTENNA POLE EXTRACTED
PREDICTED WAVEFORM
TIME (NSEC)
0.
20.
40.
60.
80.
100.
120.
140.
160.
180.
200.
VOLTAGE (MV)
-4.
-3.
-2.
-1.
0.
1.
2.
3.
4.

Figure 18c.

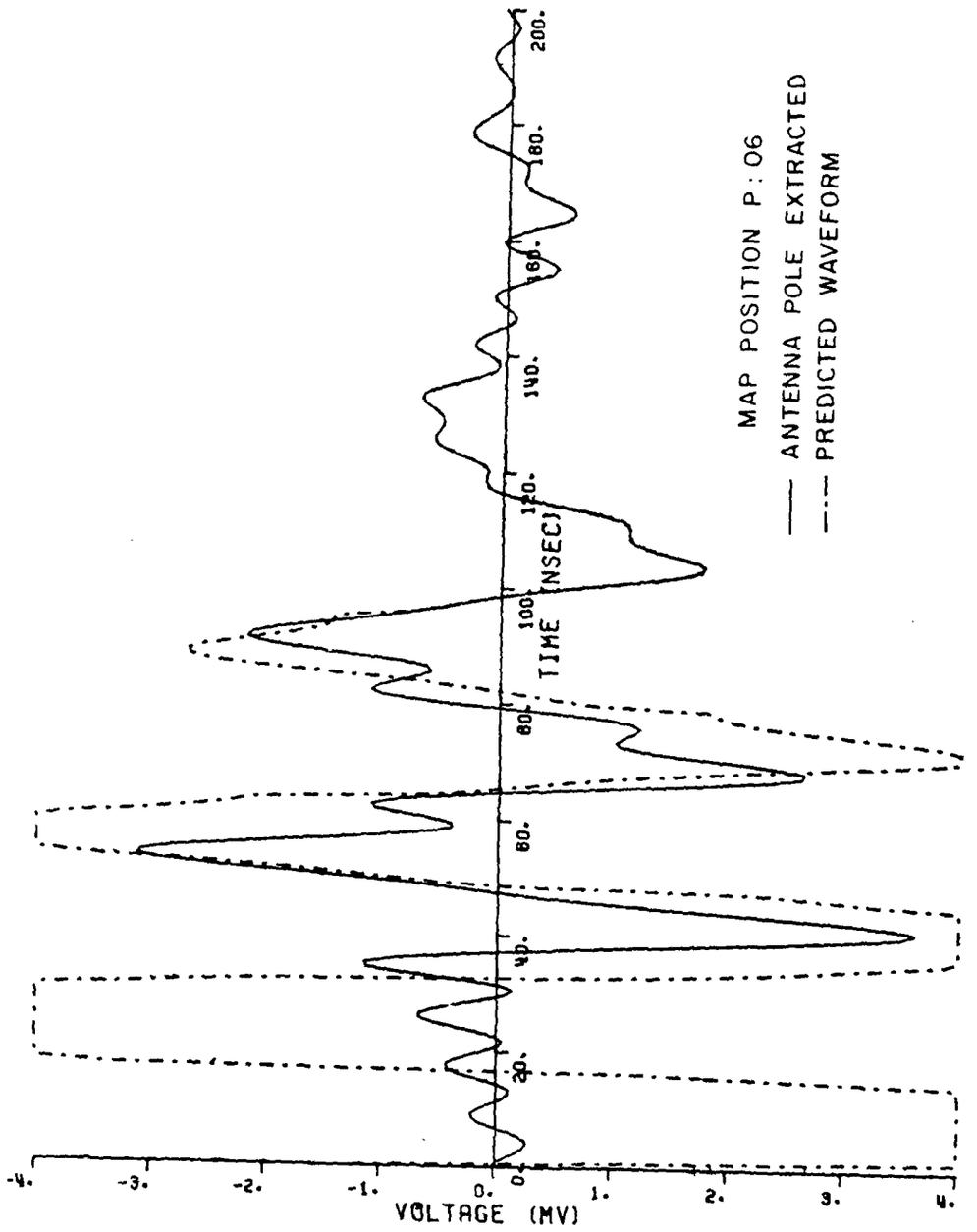
MAP POSITION P:06
ANTENNA POLE EXTRACTED
PREDICTED WAVEFORM
TIME (NSEC)
VOLTAGE (MV)
200.
180.
160.
140.
120.
100.
80.
60.
40.
20.
0.
-4.
-3.
-2.
-1.
0.
1.
2.
3.
4.

Figure 18d.

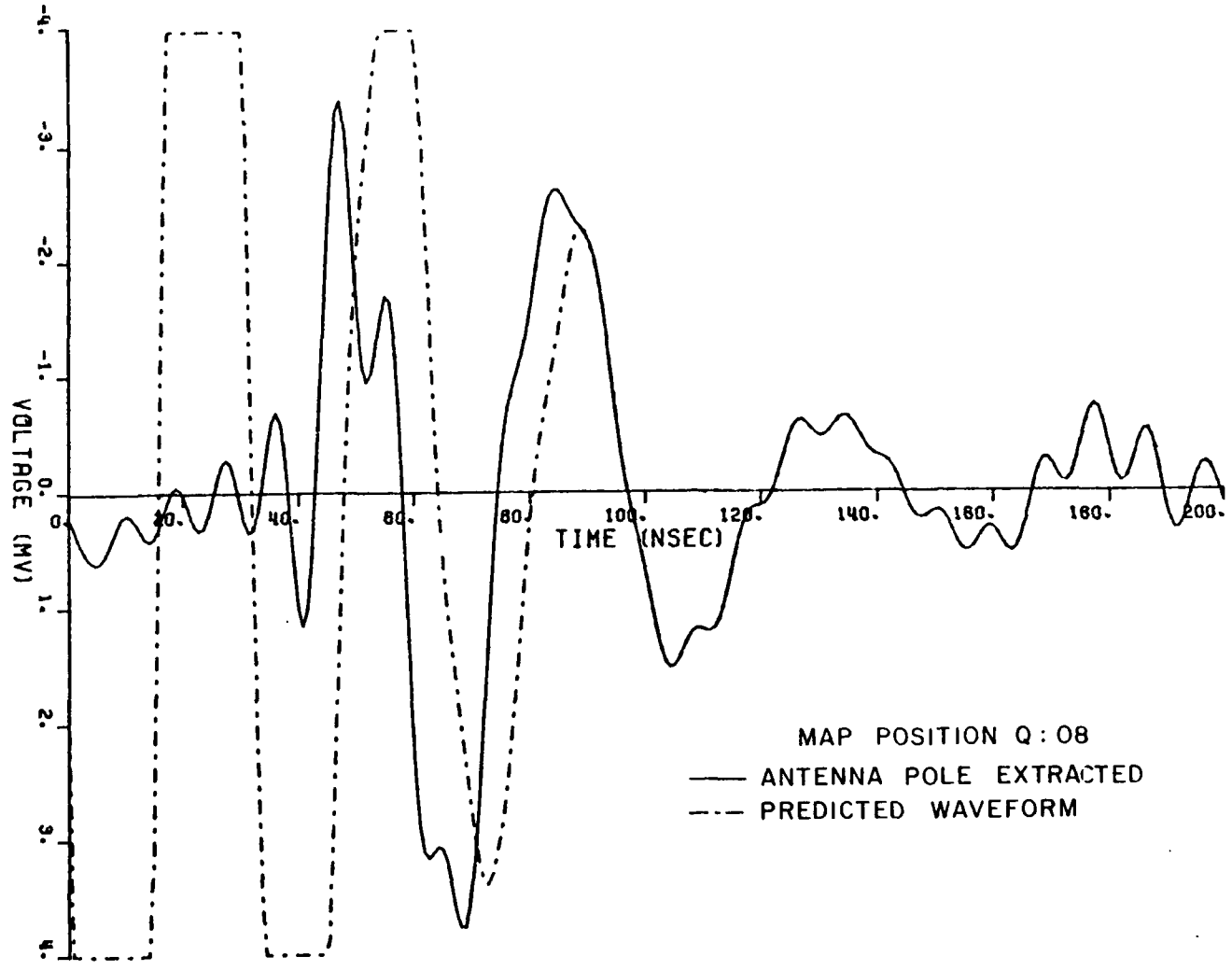
VOLTAGE (MV)
-4.
-3.
-2.
-1.
0.
1.
2.
3.
4.
0
20.
40.
60.
80.
100.
120.
140.
160.
180.
200.
TIME (NSEC)
MAP POSITION Q:08
ANTENNA POLE EXTRACTED
PREDICTED WAVEFORM

Figure 18e.

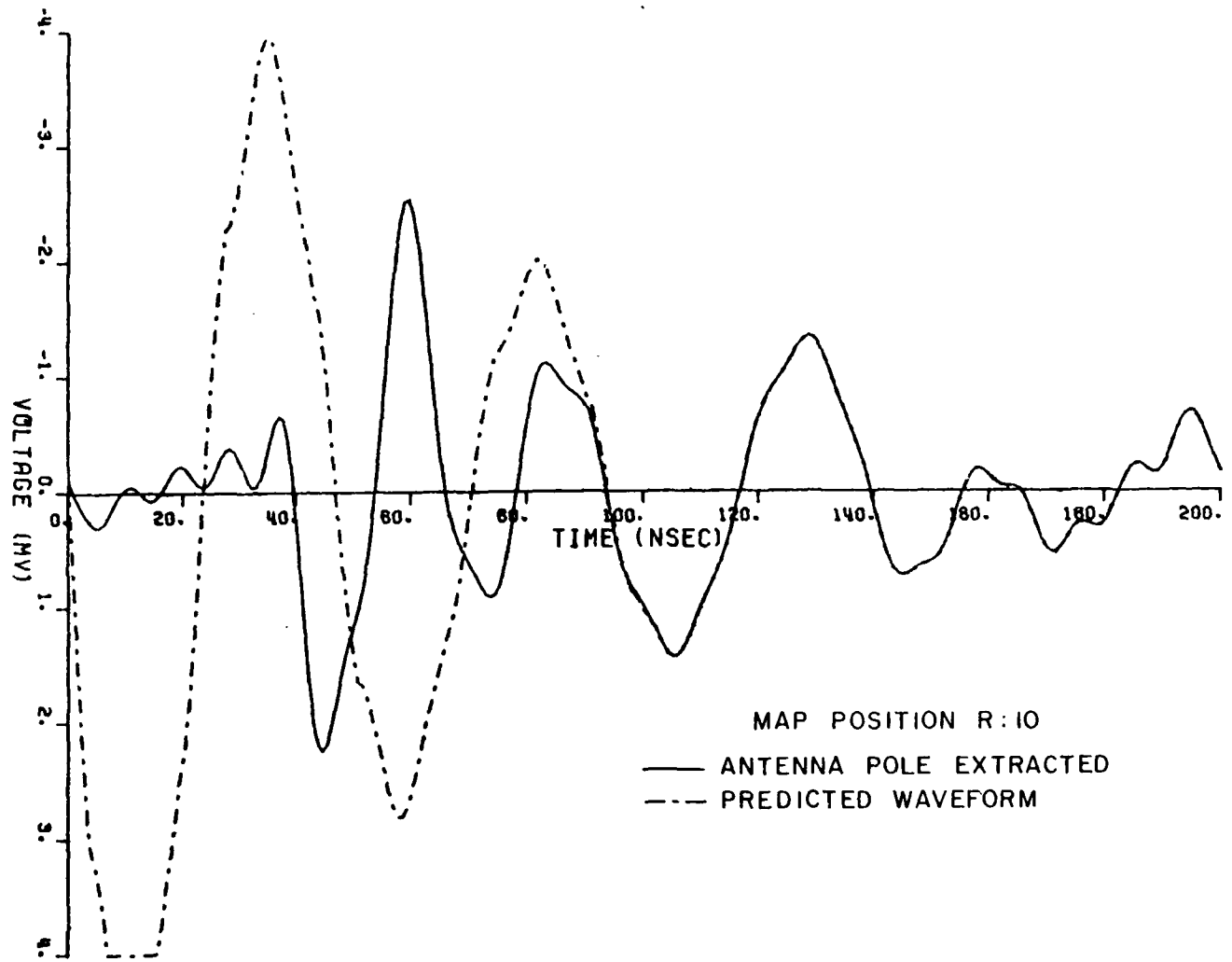
VOLTAGE (MV)
-4.
-3.
-2.
-1.
0.
1.
2.
3.
4.
0.
20.
40.
60.
80.
100.
120.
140.
160.
180.
200.
TIME (NSEC)
MAP POSITION R:10
ANTENNA POLE EXTRACTED
PREDICTED WAVEFORM

Figure 18f.

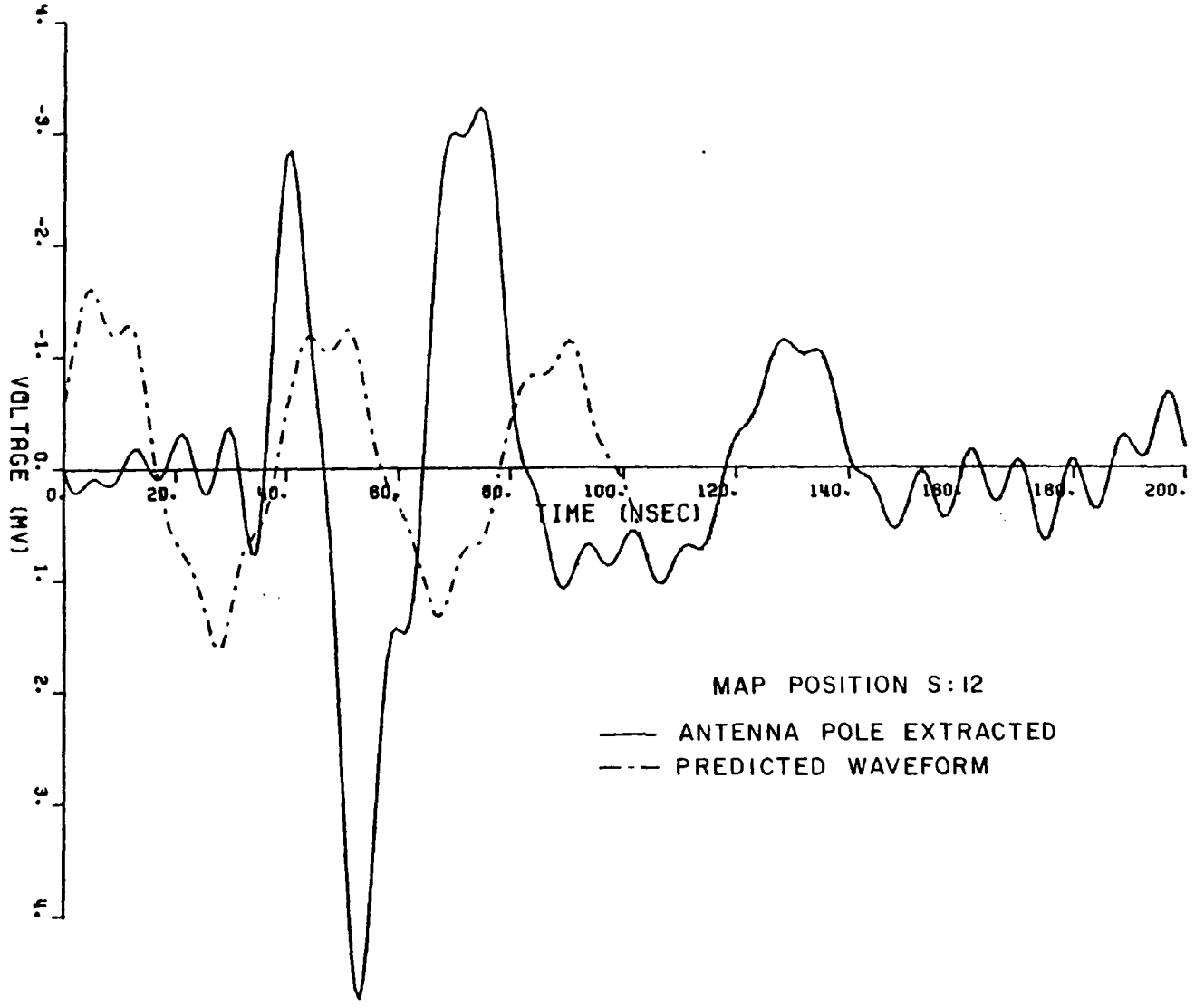
VOLTAGE (MV)
TIME (NSEC)
MAP POSITION S:12
ANTENNA POLE EXTRACTED
PREDICTED WAVEFORM

Figure 18g.

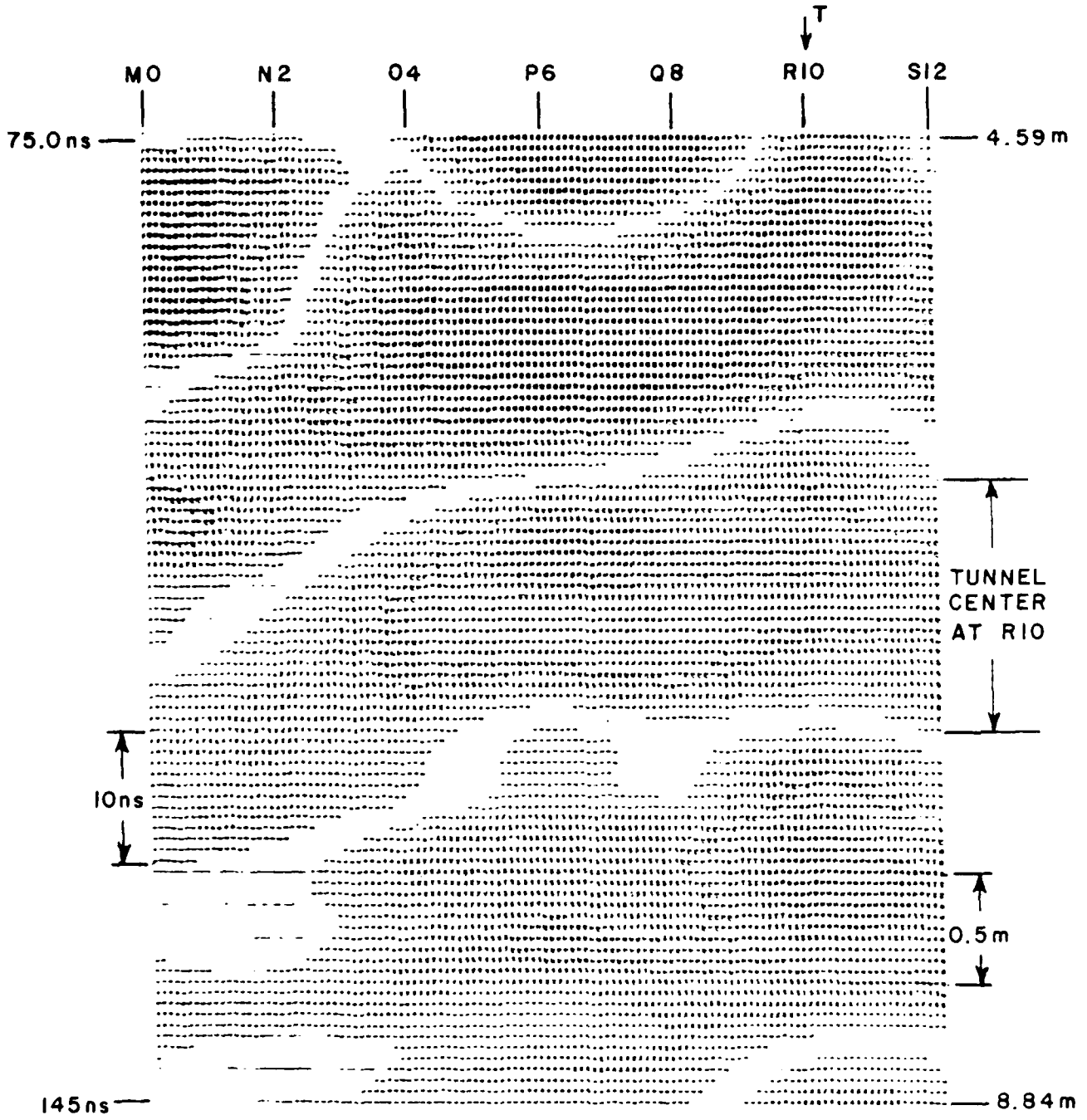

Figure 19. Grey level plot obtained using processed data from 20 foot depth above tunnel at the Hazel A Mine site. Raw waveforms were taken at 2 foot intervals transverse to the tunnel point R-10 is directly above the tunnel.

In this case we look for an appreciable segment where the solid lines and the broken lines are in agreement. This will occur if only one pole is contained in this segment of the waveform. Using this as a basis and now working with the broken curve only we march from this late time segment to the time origin. The broken curve and the solid curve will deviate at some point in time. This time coincides with the presence of the forced response from the tunnel. As is the case in ordinary circuit theory, the forced response does not contain the natural resonances and thus Equation (3) is not really applicable. It is interesting to note that in all cases of Figure 18, the two waveforms are in good agreement for times even earlier than the first null caused by the tunnel scattering. For example, for the case where the antenna directly over the tunnel (Position R-10), this first null is at approximately 95 ns whereas the waveforms are in agreement for times greater than 90 ns. This is true for all waveforms in the set except that of Position S-12. The early time remainder of the broken waveform is not valid since the scattered waveform has not arrived at the receiver at this early time. Thus the growing exponential (from $0 < t < 70$ ns) should be discarded.

There remains in this process something of a judgement factor. Specifically, where is the reconstructed waveform real and where (in early time) has it been created by the process. This question can probably be answered by convolving the predicted waveform with original measured waveform. This has not as yet been done.

The GLP shown in Figure 19 has been obtained using these predicted waveforms. Note that the result is different than the one given in Reference 7 in that it was obtained from a later data set and included additional processing.

The tunnel is clearly present at the proper place, i.e., centered at R-10 and both the top and the bottom of the tunnel are clearly indicated. The darkened area above the tunnel is introduced via the processing and can be ignored. It appears, as we have discussed earlier,

because the difference equation is trying to force a solution using a growing exponential form. It is anticipated that a detailed paper applying this process to much of the data developed under this study will be written under Contract N00014-78-C-0049 and copies will be forwarded to the MERADCOM sponsor. This process may very well be an important step in increasing the projected range at which a tunnel can be observed.

PROJECTIONS

Earlier reports[5,6] have furnished data on which equipment design can be based. It is then the intent of this section to incorporate the experimental data into the theoretical results to evaluate the depth at which this tunnel could be detected using the present equipment a) with a minimum of processing and b) with as much processing as is now deemed practical.

Next we attempt to project what could be done to improve our results and to "guess" what depths would then be practical. First we observe here that the tunnel was clearly detected with a peak return signal level of about 10 mv at a depth of 20 feet. Cable and balun losses were measured to be about 18 dB in these experiments so assuming a nominal 1000 v pulser, this is equivalent to a 130 v transmitter provided both it and the receiver were placed directly at the terminals of the antenna as has been verified by experiment. This can be nearly accomplished. Using the present receiver, one can increase the sensitivity to observe a voltage waveform as small as ½ mv. Thus the present equipment is capable of observing a signal that is 44 dB below that obtained for this tunnel at 20 feet in the absence of clutter. We hope that the processing scheme discussed in this report could eventually reduce the significance of such clutter. We now assume the conductivity of the granite medium to be 0.002. We have presented a plot of the attenuation function A_f in Figure 26 of Reference 5. For the case we

are discussing, the value of A_F ~ 34 dB. Adding the projected 44 dB, the range at which the tunnel could be detected using the present equipment would be about 60 feet.

There are two potential ways in which equipment can be improved. One of these would be to increase the sensitivity of the receiver transmitter system in some way or another. There are wide band amplifiers available that would be appropriate. The output level of the pulser can also be increased. Let us assume that approximately 50 dB is practical. Then the projected range would be increased to approximately 100 feet. Observe however a large increase in system sensitivity is needed to double the effective range.

We must caution the reader that much care must go into the design and the application of such a system. It is also assumed that clutter is not a limiting factor and research must be directed toward eliminating the effects of clutter. The techniques that we have just introduced need to be thoroughly researched.

There is also the possibility of increasing the length of the antenna system. This is discussed in a companion report but it is observed that the limit where an HFW radar may be used has been reached (see Figure 6 of Reference 5). Furthermore, the LBANT antenna spectral characteristics already reasonably match those of the tunnel.

All of the above data is based on the use of a single antenna element or a crossed transmit/receive pair. There is also the possiblility that an array could be used to focus energy on the target. Let us now assume a very complex array system is developed, say a 10 element array with 10 triggerable pulsers and 10 coherent receivers whose voltage output can be summed. This would give an increase in signal level of 40 dB and the detectable target range is only increased to 130 feet. This represents a tremendous increase in technology with only marginal increase in maximum range.

There remains the possibility of operating in the LFW. However, at the Gold Hill site for the measurements discussed in this report the depth is too shallow and the tunnel resonance too high in frequency for this mode of operation. This will be discussed further in a companion report where a wire has been included in the tunnel[3].

CONCLUSIONS

Based on our original theoretical studies[5,6], a Video Pulse radar system was designed and operated in a HFW radar mode. The equipment was successfully operated both at the Hazel A mine outside of Gold Hill, Colorado and at abandoned coal mine sites under Curtis School Yard in Trumbull County, Ohio. This report has documented the data and the conclusions generated by the Gold Hill data using the modified Terrascan Antenna and the Long Box Antenna. Companion reports will document comparable data from the Curtis School and also data obtained using a Long Balun Feed Antenna system (LBFA).

The tunnel at Gold Hill can be entered and an antenna mounted against its roof. Propagation measurements from antennas inside the tunnel to antennas on the surface have given a good estimate of the permittivity. Similar attempts to monitor the conductivity have not been so successful.

The tunnel at depths up to 20 feet have been detected using the HFW radar system in this granite media. It is projected that by careful design and careful measurements that tunnels at depths of 100 feet could be detected in this granite media.

A processing technique has been introduced that greatly improves the signal to clutter levels. The experimental data so processed has been used to create a grey level plot for a set of measurements. The grey level plot clearly shows the tunnel at about the correct position. Other grey level plots without such processing did indeed reveal the presence of the tunnel but the results were not nearly as obvious as

in the final grey level plot. This new processing technique should be developed further and indeed this is a necessity if the projected 100 foot detection range is to be achieved on a routine basis.

The data in this report is probably inadequate to really verify with 100% confidence all of the conclusions based upon it. It is suggested that this site is nearly ideal and that a substantial measurement program extending over a much longer time period should be made.

The equipment developed under this study has gone through several stages of development. However there are areas where further improvements can be made. Some of these have already been discussed but there still appears to be a need for further antenna development and further pulser improvement. With respect to the pulser, it may be practical to simplify the system response by using a periodic step (long pulse) so that reflections associated with only one discontinuity of the transmitted signal (the rising edge) be contained in the range window. A third improvement would be to introduce a means of increasing the system gain for targets of greater depth. This might take the form of an exponential increase in gain as a function of time in order to negate the exponential decay caused by ground losses.

ACKNOWLEDGMENTS

The authors are most grateful to Mr. Richard Myers for his assistance in gaining access to the Gold Hill mine site. The authors are also indebted to Mr. Luen Chan and Mr. John Volakis for their assistance in developing the new data processor. The authors are indeed indebted to Professor E. M. Kennaugh whose original work in similar data processors suggested the present scheme. His suggestions have also been very helpful. Dr. J. D. Young has contributed significantly to the techniques used to obtain the experimental data.

REFERENCES

References 1, 2, 3, 5, 6, 7, 8, and 9 were prepared by The Ohio State University ElectroScience Laboratory, Department of Electrical Engineering under Contract DAAG53-76-C-0179 for U. S. Army Mobility Equipment Research and Development Command, Ft. Belvoir, Virginia.

1. C. W. Davis, III and L. Peters, Jr., "Summary of Studies on Tunnel Detection Radar System," Final Report 784460-11, January 1979.

2. C. W. Davis, III and R. Gaglianello, "A Video Pulse Radar System for Tunnel Detection," Report 784460-9, January 1979.

3. C. W. Davis, III and L. Peters, Jr., "The Preliminary Development and Application of a Long Balun Fed Antenna for Video Pulse Radars," Report 784460-10, January 1979.

4. D. L. Moffatt and R. J. Puskar, "A Subsurface Electromagnetic Pulse Radar," Geophysics, Vol. 41, No. 3, June 1976, pp. 506-518.

5. G. A. Burrell, L. Peters, Jr., A. J. Terzuoli, Jr., "The Propagation of Electromagnetic Video Pulse with Application to Subsurface Radar for Tunnel Application," Report 784460-2, December 1976.

6. L.Peters, Jr., G. A. Burrell, H. B.Tran, "A Scattering Model for Detection of Tunnels Using Video Pulse Systems," Report 784460-3, February 1977.

7. D. O. Stapp, "Method for Grey Scale Mapping of Underground Obstacles Using Video Pulse Radar Return," Report 784460-5, December 1978.

8. L. A. Wald, "Modification of the HFW Underground Antenna Based on Experimental Studies," Report 784460-6, January 1979.

9. C. A. Tribuzi, "An Antenna for Use in an Underground (HFW) Radar System," Report 784460-4, November 1977.

END

DATE

FILMED

DTIC

10-88